FORMATION CONTROL FOR COOPERATIVE SURVEILLANCE

A Dissertation

by

SANG-BUM WOO

Submitted to the Office of Graduate Studies of
Texas A&M University
in partial fulfillment of the requirements for the degree of

DOCTOR OF PHILOSOPHY

December 2008

Major Subject: Mechanical Engineering

FORMATION CONTROL FOR COOPERATIVE SURVEILLANCE

A Dissertation

by

SANG-BUM WOO

Submitted to the Office of Graduate Studies of
Texas A&M University
in partial fulfillment of the requirements for the degree of

DOCTOR OF PHILOSOPHY

Approved by:

Chair of Committee,	Suhada Jayasuriya
Committee Members,	Alexander Parlos
	Reza Langari
	Shankar P. Bhattacharyya
Head of Department,	Dennis O'Neal

December 2008

Major Subject: Mechanical Engineering

ABSTRACT

Formation Control for Cooperative Surveillance. (December 2008)

Sang-Bum Woo, B.S., Yonsei University;

M.S., Texas A&M University

Chair of Advisory Committee: Dr. Suhada Jayasuriya

Constructing and maintaining a formation is critical in applications of cooperative control of multi-agent systems. In this research we address the formation control problem of generating a formation for a group of nonholonomic mobile agents. The formation control scheme proposed in this work is based on a fusion of leader-follower and virtual reference approaches. This scheme gives a formation constraint representation that is independent of the number of agents in the formation and the resulting control algorithm is scalable. One of the important desired features in controller design is that the formation errors defined by formation constraints should be stabilized globally and exponentially by the controller. The proposed controller is based on feedback linearization, and formation errors are shown to be globally exponentially stable in the sense of Lyapunov. Since formation errors are stabilized globally, the proposed controller is applicable to both formation keeping and formation construction problems. As a possible application, the proposed algorithm is implemented in a cooperative ground moving target surveillance scenario. The proposed algorithm enables the determination of the minimal number of agents required for surveillance of a moving target. The number of agents returned by this scheme is not optimal and hence is a conservative solution. However, this is justified by the computational savings the scheme offers.

To my parents and my wife Hyunjung

ACKNOWLEDGMENTS

I would like to express my gratitude to a number of people without whom it would have been impossible to complete this dissertation.

First of all, I would like to express special thanks to my advisor, Dr. Suhada Jayasuriya for his guidance and support throughout my Ph.D. program. His academic excellence and good personality have provided a constant source of encouragement.

With great pleasure, I wish to extend my sincere thanks to Dr. Alexander Parlos, Dr. Reza Langari, and Dr. Shankar P. Bhattacharyya who willingly agreed to be on my graduate committee in spite of their busy schedule and have made valuable comments on my research work.

I would like to extend my deepest gratitude to my parents and wife, Hyunjung who have always supported me and shown their unselfish love.

TABLE OF CONTENTS

CHAPTER Page

LIST OF TABLES

LIST OF FIGURES

CHAPTER I

INTRODUCTION

A. Formation Control Problem

Extensive research has been conducted on cooperative control for multi-agent systems in the past decades. Since multi-agent systems can overcome physical limitations of single agent capabilities, they are superior to single agent systems when they are deployed in cooperative tasks such as exploring and mapping hazardous terrains [1], searching environments [2], and conducting surveillance of moving targets [3].

In order to accomplish multiple tasks, they need to be allocated to each agent in the multi-agent system. This process is the first step for such a system to fulfill a task. Next, data are exchanged through communication between neighboring agents. The final step is to coordinate the agents in the system to reach their desired positions. The task allocation problem is also known as the assignment problem. Each task can be assigned to the proper agent by linear optimization [4] or by a distributed algorithm with low ratio bounds [5]. One of the key issues in information flow is to determine the effect of communication failures and delays between agents on formation stability. Fax and Murray [6] determines this effect by the eigenvalues of the graph Laplacian matrix.

After all tasks are already allocated effectively and efficiently, and each agent has the required data for group tasks, a control strategy is required for the collaboration of the team of agents. The following has been considered in the literature in the control design step: maintaining geometric relationship between agents, dynamic constraints, and avoiding inter agent collision. Maintaining geometric relationship between agents

---

The journal model is *IEEE Transactions on Automatic Control.*

has been covered through formation control in the literature. For instance, box pushing problem in [7], load transportation in [8], and formation flight in [9, 10] require the agents to maintain a certain distance between each other. This geometric relationship appears as constraints or control objectives in control design. Dynamic constraints relate to the agent platforms. Since most actual agents are wheel-based, nonholonomic constraints in dynamics have often been considered for multi-agent system in the literature. While nonholonomic constraints capture the features of wheel-based agents well, it makes designing a controller challenging. Avoiding collision between agents has been considered in changing geometric relationships among agents or in maintaining a fixed geometric relationship. For some applications such as search and rescue [2], and surveillance [3], the desired path of each agent depends on the target movement. If the target moves randomly, motion planning or path planning is not an option. Therefore, approaches for collision avoidance based on path planning such as the cell decomposition approach [11, 12] are not directly applicable to a problem involving randomly moving targets.

B. Previous Work in the Literature

In this dissertation we are interested in the formation generating problem. The formation generating problem is similar to formation keeping except, that formation errors are stabilized globally instead of locally. The key issue in formation generating is the design of a control law for each agent such that all agents fall within a preassigned formation. Designing such a control law for each agent requires the reference position for each of the agents. Some approaches to deciding the reference position in the literature assume that the reference trajectory for agents is known a-priori rather than computed in real-time. This approach may not be suitable when the shape and the

motion of the formation are dependent on the group objectives or tasks. Designing reference position in real-time is typically specified roughly by three methods in the literature: leader-follower, neighbor reference, and virtual reference.

The leader-follower approach is used for the formation generating problem in [13, 14, 15]. A single agent can be designated as a leader [15], or there can exist multiple leaders [13, 14]. The desired position of the follower in the preassigned formation is simply decided by a geometric relation between the leader and its followers. A drawback of the leader-follower approach is that the group behavior highly depends on the physical constraints of leaders. The leader-follower approach to formation control can be exceptionally challenging when the group has to undergo rotational motion. The geometric constraints between a leader and its followers need to be modified whenever there is a difference between the linear velocity direction of the leader and that of the group formation. Another drawback of the leader-follower reference approach is that the formation stability is highly dependent on the leaders. The weakness of the leader-follower approach at times can also be an advantage. Namely, the group behavior can be directed by just the behavior of leaders.

In the neighbor reference approach, each agent makes an effort to decrease the formation error [16]. Since there is no explicit reference point or frame in the latter, it is challenging to guide the formation. But, this approach is suitable for decentralized, autonomous control. This approach does not require a global reference point, and each agent can make a preassigned formation without central communication.

The virtual reference approach involves what we term the virtual structure(**VS**) concept. The virtual reference point is computed by averaging the positions of all the agents in [17], or the virtual reference frame can be fixed at the virtual center of the formation, or at the center of the **VS** as in [9, 18]. The main strength of the virtual reference approach is that the guidance of a group is easier than the other

approaches since all agents in the formation are treated as a single object. However, the physical constraints of each of the agents do not appear explicitly in the group behavior. Therefore, it is a challenging problem to meet control bounds of each agent with the virtual reference approach. Another drawback is that the virtual reference approach introduces non-scalability in computation. The computational time increases exponentially with the number of agents, and adding just one agent to the formation results in a recalculation of the formation errors and the control law. In this dissertation we study the formation forming problem using a mixture of the leader-follower and the virtual reference methods in order to overcome the above drawbacks.

C. Our Contribution

The main goals of this research have been to develop control laws to specify the motion of multi-agent systems to achieve cooperative tasks. The work in this dissertation is aimed at achieving the goals by completing the following objectives.

- Develop a scalable scheme for generating a formation.
- designed controllers stabilize formation errors globally even when uncertainties exist in the system model.
- Design a real-time algorithm which utilizes a minimal number of agents for the surveillance problem.

One of our contributions in this research is the development of a scalable scheme for formation construction. The proposed scheme is based on a novel expression of rigid formation and formation constraints. The desired features for scalability in the formation constraints are:

- The number of constraints are a multiple of N when the formation is composed of N actual agents.
- The position information of one agent in a given formation should appear in just one formation constraint tied to the agent.

These features are achieved by introducing virtual agents in the proposed scheme. The virtual agents not only make the formation constraints meet the desired features but also lend itself to formation guidance. Another advantage of the proposed scheme appears in the motion of the resulting formation. Since the orientation of virtual or actual agents do not coincide with the orientation of the formation, the motion of the formation is independent of a path curvature. The seconde contribution of this research is in that the proposed controllers stabilize the formation errors globally and exponentially. The formation error dynamics is constructed by the proposed scalable algorithm, and linearized by feedback. Another controller is proposed in order to avoid matrix inversion in computation. By nonlinear mapping, the formation composed of nonholonomic agents can be stabilizable even when the formation is stationary. Since there is no matrix inversion in computing the control law, complexity in computation will not occur. A controller stabilizing the formation errors in the presence of model uncertainty is considered by Lyapunov redesign method. Asymptotic stability of the formation errors is shown. Last, a surveillance scheme is developed for multi-agent systems. A minimal number of agents and their distribution are determined by the proposed scheme to monitor a moving target. The computation requires only controller bounds of agents and it is independent of the number of agents N, while the algorithms based on optimization technique have order of N^N time complexity [5]. Therefore, computation time is much shorter than other algorithms based on optimization techniques.

D. Organization

First, we define a formation, rigid formation, and formation constraints in chapter I. Then, we discuss scalable formation constraints and controller design based on feedback linearization in chapter II. In chapter III, we discuss practical issues which appear in actual applications. Cooperative surveillance of a moving target problem is considered in the formation framework in chapter IV. Concluding remarks and future work are given in chapter V.

CHAPTER II

CONSTRUCTING A FORMATION

A. Preliminaries

Formation control has been researched for decades: In 1989, Wang [15] studied formation generation with point-mass type agents. In the 1990's, formation control was researched via the virtual structure(**VS**) concept. In the latter a virtual reference point is computed by averaging the positions of all the agents as in [17], or a virtual reference frame can be fixed at a virtual center of the formation as in [18]. In early 2000's, attention was shifted to distributed algorithms; For example in [19, 20] considered was the objective of getting a group of agents to assemble at a common location which has come to be known as the rendezvous problem. In 2004, the effect of communication failures and delays between agents on formation stability was studied in [6]. Recently, formation guidance and formation keeping problem with nonholonomic agents was considered in [21, 22, 23]. However, it is hard to find the definition of a formation. Also, the meaning of a formation is different from one to another. For example, the concept of a formation introduced in [13] includes the orientation of agents, while the notion of a formation in [18] does not. In order to avoid such misconceptions, a definition of a formation is required before further discussion.

1. Definition of Formation

We define a formation as follows:

Definition 1 (Formation) *Let us assume that N rigid body agents(robots or vehicles) are assigned to get into a certain formation. Let the mass center of the i^{th} agent be denoted by position vector $\boldsymbol{r}_i(t)$. Let $[\ ]_A$ denote the coordinates of a vector in a*

frame A. Then, the set

$$F = \{[\boldsymbol{r}_1(t)]_A, [\boldsymbol{r}_2(t)]_A, \cdots, [\boldsymbol{r}_N(t)]_A\}$$

at a given time t is said to be the formation at time t.

By this definition, only positions of agents affect the configuration of a formation. Namely, the individual orientations of agents in a formation has no effect on the configuration of the formation.

Definition 2 (Rigid Formation) *A formation F is a rigid formation if there exist a positive-definite orthogonal matrix $\boldsymbol{R}(t)$ and a vector $\boldsymbol{d}(t)$ at time t such that $[\boldsymbol{r}_i(t)]_A = \boldsymbol{R}(t)[\boldsymbol{r}_i(t_0)]_A + [\boldsymbol{d}(t)]_A$ for $i = 1, 2, \cdots, N$ and $t \in [t_0, t_f]$.*

Remark 1 *If $\boldsymbol{R}(t)$ is a negative-definite orthogonal matrix, then the shape of the formation will be flipped.*

In general, constructing a certain formation means forming a rigid formation from a non-rigid formation.

Remark 2 *The distance $d_{i,j} = |r_i(t) - r_j(t)|$ will be maintained for time $t \in [t_0, t_f]$ if the formation is rigid.*

Definition 3 (Virtual Structure) *A rigid formation may be assumed to be a single virtual rigid body, and this rigid body is called a virtual structure(**VS**).*

2. Degrees of Freedom

If all the agents are assumed to be rigid bodies in n dimensions, a formation composed of N agents has nN degrees of freedom(**DOF**)s. Since a flipped shape may not be allowed in transformation by translation and rotation, the number of **DOF** of a rigid

formation is the same as that of a rigid body. Therefore, a rigid formation composed of N agents has only $\frac{n(n+1)}{2}$ **DOF**s. In other words, at least $nN - \frac{n(n+1)}{2}$ constraints are required for a rigid formation composed of N agents. Let us call these constraints *formation constraints.*

Definition 4 (Formation Constraints)

$$Q_j([\boldsymbol{r}_1^*(t)]_I, [\boldsymbol{r}_2^*(t)]_I, \cdots, [\boldsymbol{r}_N^*(t)]_I) = 0$$

are formation constraints for $j = 1, \cdots, k(\geq nN - \frac{n(n+1)}{2})$ *in* $\mathcal{R}^n$*, and* $Q_j = 0$ *are sufficient for the formation* $F = \{[\boldsymbol{r}_1(t)]_I, [\boldsymbol{r}_2(t)]_I, \cdots, [\boldsymbol{r}_N(t)]_I\}$ *to be a rigid formation, where* $[\boldsymbol{r}_i^*(t)]_I$ *is the desired position of* i^{th} *agent in a rigid formation.*

When there is an error between the position of i^{th} agent and the desired position of i^{th} agent in a formation, we call it a *formation error.*

B. Problem Statement

Suppose N agents are assigned to construct a specified rigid formation $F = \{[\mathbf{r}_1^*(t)]_I, [\mathbf{r}_2^*(t)]_I, \cdots, [\mathbf{r}_N^*(t)]_I\}$, and suppose that the motion of each agent is governed by the following state equations;

$$\begin{aligned} \dot{\mathbf{z}}_i &= f_i(\mathbf{z}_i) + g_i(\mathbf{z}_i)\mathbf{u}_i \\ \mathbf{r}_i &= h_i(\mathbf{z}_i) \end{aligned} \tag{2.1}$$

where $i = 1, 2, \cdots, N$, $\mathbf{z}_i \in \mathcal{R}^n$ is the state of the i^{th} agent, $\mathbf{u}_i \in \mathcal{R}^p$ is the control for the i^{th} agent, $\mathbf{r}_i$ is the position vector of the i^{th} agent with respect to an inertial frame. In this chapter we design the controller, $\mathbf{u}_i(t)$ such that $\lim_{t\to\infty} \sum_i^N \|\mathbf{r}_i^* - \mathbf{r}_i\| = 0$.

1. Assumption

The first assumption is that each agent is able to calculate its global position $[\mathbf{r}(t)]_I$, and is able to determine the desired position in a specified rigid formation $[\mathbf{r}^*(t)]_I$ at any time. As a preliminary step, we assume that there is no collision among agents, although it can be handled by the potential field approach.

C. Approach for Scalability

As we discussed in the previous chapter, defining a desired position of each agent is the key to constructing a formation. Now we introduce a new approach which is based on a blend of the virtual reference approach and the leader-follower approach. Let us assume the assigned rigid formation is a virtual rigid body, which we call virtual structure(**VS**). A local frame B is assumed fixed to the **VS** with its origin O_B. $\mathbf{b}_i$ is the position vector of the i^{th} agent with respect to O_B. $\mathbf{r}_i$ is the position vector of the i^{th} agent with respect to an inertial frame I, and $\mathbf{r}_i^*$ is the position vector of the desired position of i^{th} agent with respect to an inertial frame I.Let $[\#]_B$ denote the coordinates of a vector in the local frame B and $[\#]_I$ denote the coordinates of a vector in an inertial frame I. The position of each of the agents can be specified by $\mathbf{b}_i$ which is shown in Fig.1.

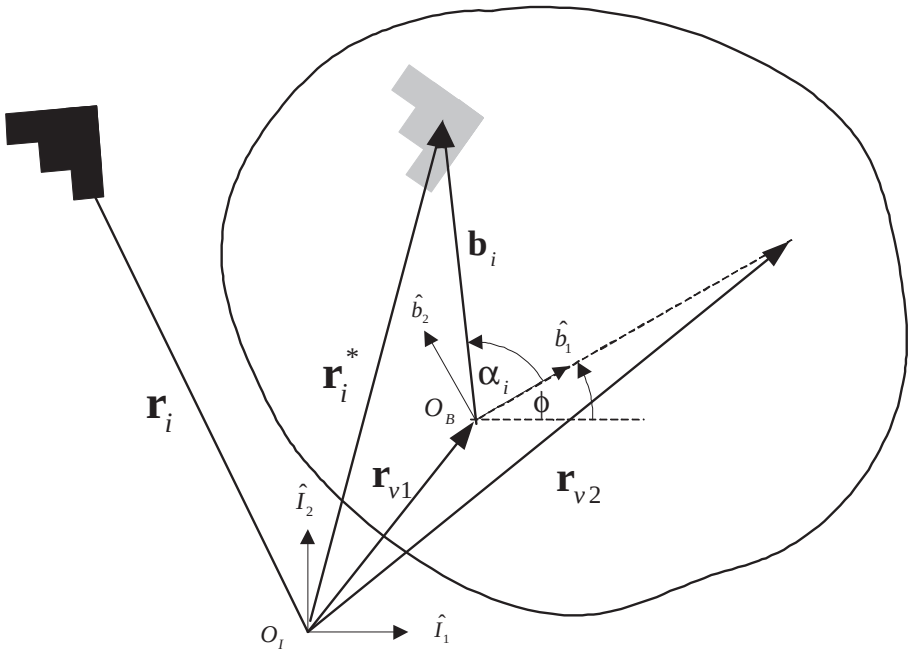

Fig. 1. Configuration of formation in $\mathcal{R}^2$

D. Constraints and Errors

Definition 5 (Function $\angle$)

$$\angle\left(\begin{bmatrix} x \\ y \end{bmatrix}\right) = \begin{cases} \arctan(y/x), & for\ x > 0 \\ \arctan(y/x) + \pi, & for\ y \geq 0, x < 0 \\ \arctan(y/x) - \pi, & for\ y < 0, x < 0 \\ \frac{\pi}{2}, & for\ y > 0, x = 0 \\ -\frac{\pi}{2}, & for\ y < 0, x = 0 \\ undefined, & for\ y = 0, x = 0 \end{cases}$$

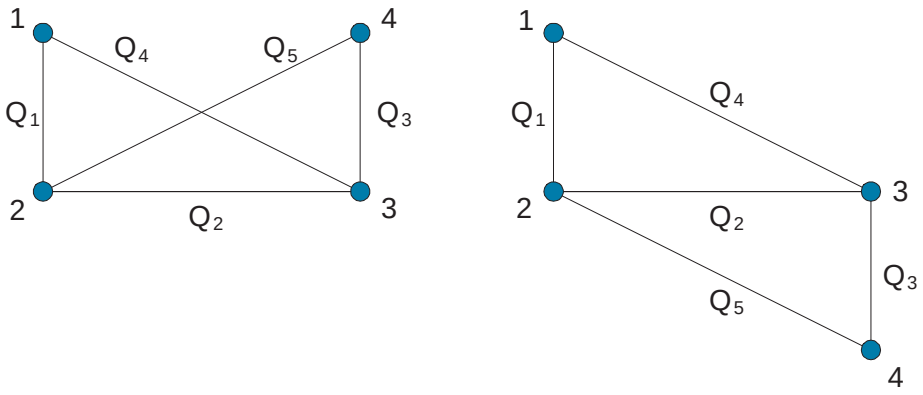

Fig. 2. Non-sufficient formation constraints

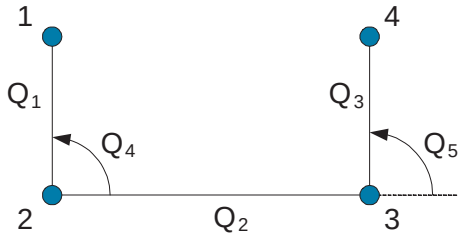

Fig. 3. Sufficient formation constraints

One can suggest the following formation constraints in $\mathcal{R}^2$;

$$Q_i = \begin{cases} \|\mathbf{r}_i^* - \mathbf{r}_{i+1}^*\|^2 - d_{i,i+1}^2 = 0, & \text{for } i = 1,\ldots,N-1 \\ \|\mathbf{r}_{i-N+1}^* - \mathbf{r}_{i-N+3}^*\|^2 - d_{i-N+1,i-N+3}^2 = 0, & \text{for } i = N,\ldots,2N-3 \end{cases} \tag{2.2}$$

where $d_{a,b}$ is the desired distance between the a^{th} agent and the b^{th} agent, and the desired position of the i^{th} agent is denoted by $\mathbf{r}_i^*$. These $2N-3$ constraints are not enough to specify one shape of formation although the number of constraints satisfies requirements of formation constraints. Figure 2 shows possible rigid formations with the constraint represented by Eq.(2.2). The representation of formation constraints

in Eq.(2.2) may be replaced by the following;

$$Q_i = \begin{cases} \|\mathbf{r}_i^* - \mathbf{r}_{i+1}^*\|^2 - d_{i,i+1}^2 = 0, & \text{for } i =_{1,\ldots,N-1} \\ \angle([\mathbf{r}_{i-N+1}^* - \mathbf{r}_{i-N+2}^*]_I) - \angle([\mathbf{r}_{i-N+3}^* - \mathbf{r}_{i-N+2}^*]_I) \\ \qquad -\alpha_{i-N+1,i-N+3} = 0, \quad \text{for } _{i=N,\ldots,2N-3} \end{cases}$$

where $\alpha_{a,a+2}$ is the desired angle between the two vectors, $\mathbf{r}_a^* - \mathbf{r}_{a+1}^*$ and $\mathbf{r}_{a+2}^* - \mathbf{r}_{a+1}^*$. These $2N-3$ constraints shown in Fig.3 are sufficient to specify the formation, however, each agent is connected to each other in sequence through intermediate agents. Namely, the constraint Q_k is not independent of the constraint Q_{k-1}. Consequently, this formalism is not scalable. Another idea for realization of formation constraints is given in [24]. Here the formation constraints were defined through a single function. However, this representation depends on the number of agents. Therefore we need to find a new representation of formation constraints which satisfies the following conditions;

- The number of formation constraints should be a multiple of N when the formation comprises N actual agents.
- Each formation constraint should be represented by the configuration of only one agent.

By introducing virtual leaders, formation constraints can be made independent of each other, thereby making the formalism for formation generation scalable in the number of agents. Another advantage of introducing virtual leaders is that the behavior of the specified rigid formation can be directed by just the behavior of virtual leaders. One can choose new constraints for the formation, which contains two virtual leaders

$\mathbf{VL}_1$, $\mathbf{VL}_2$, as follows:

$$\begin{aligned} Q_i &= \begin{bmatrix} \|\mathbf{r}_i^* - \mathbf{r}_{v1}\|^2 - d_i^2 \\ \angle([\mathbf{r}_i^* - \mathbf{r}_{v1}]_I) - \angle([\mathbf{r}_{v2} - \mathbf{r}_{v1}]_I) - \alpha_i \end{bmatrix} \\ &= \begin{bmatrix} q_{i,l} \\ q_{i,\theta} \end{bmatrix} = 0, \qquad i = 1, \ldots, N \end{aligned} \tag{2.3}$$

where $\mathbf{r}_{v1}$ and $\mathbf{r}_{v2}$ denote the position vectors of $\mathbf{VL}_1$ and $\mathbf{VL}_2$ with respect to the O_I in Fig.1 respectively. Hence this representation of formation constraints satisfies the two required conditions discussed above. The errors in formation are defined by substituting $\mathbf{r}_i$ for $\mathbf{r}_i^*$ in the formation constraints as follows:

$$\begin{aligned} \mathbf{E}_i &= \begin{bmatrix} \|\mathbf{r}_i - \mathbf{r}_{v1}\|^2 - d_i^2 \\ \angle([\mathbf{r}_i - \mathbf{r}_{v1}]_I) - \angle([\mathbf{r}_{v2} - \mathbf{r}_{v1}]_I) - \alpha_i \end{bmatrix} \\ &= \begin{bmatrix} e_{i,l} \\ e_{i,\theta} \end{bmatrix}, \qquad i = 1, \ldots, N \end{aligned} \tag{2.4}$$

E. Controller Design

Sliding mode control can be used for stabilizing formation error as in [25, 26]. Sliding mode control has the feature that it is robust to small disturbances, although the control law suffers from chattering [27]. In [25] the formation error is stabilized asymptotically even when the target changes its moving direction suddenly. However, the algorithm there cannot be expanded to more than two agents. In this dissertation, we propose a scheme which is applicable to $N(\geq 1)$ agents and which is also scalable. Potential field methods can lead to collision-free control laws for each agent [28]. However, it is quite challenging to incorporate nonholonomic constraints in a potential field method. Since nonholonomic constraints capture the limitation of actual agents

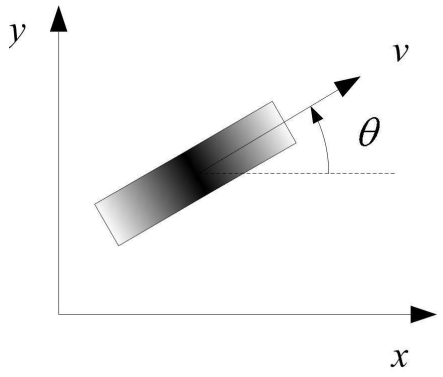

$$\begin{bmatrix} \dot{x} \\ \dot{y} \\ \dot{\theta} \\ \dot{v} \end{bmatrix} = \begin{bmatrix} v\cos\theta \\ v\sin\theta \\ 0 \\ 0 \end{bmatrix} + \begin{bmatrix} 0 & 0 \\ 0 & 0 \\ 1 & 0 \\ 0 & 1 \end{bmatrix} \begin{bmatrix} \omega \\ u \end{bmatrix}$$

Fig. 4. Unicycle model

well, for example the no slip constraints of ground vehicles, we consider nonholonomic constraints in the formalism of the approach. However this introduces nonlinearities into the control design.

1. 2D Dynamic Model of Agent

We now consider a unicycle model shown in Fig.4 for each agent. Each agent has to satisfy the nonholonomic constraint $v_i \cos\theta_i - v_i \sin\theta_i = 0$. Following the representation of Eq.(2.1), $\mathbf{z}_i = [x_i, y_i, \theta_i, v_i]^T$, $f_i(\mathbf{z}_i) = [v_i \cos\theta_i, v_i \sin\theta_i, 0, 0]^T$, $g_i(\mathbf{z}_i) = \begin{bmatrix} 0,0,1,0 \\ 0,0,0,1 \end{bmatrix}^T$, $h_i(\mathbf{z}_i) = [x_i, y_i]^T$, $\mathbf{u}_i = [\omega_i, u_i]^T$, and $\mathbf{y}_i = [x_i, y_i]^T$. Namely, the following form represents the dynamics of the i^{th} agent.

$$\begin{cases} \dot{x}_i = v_i \cos\theta_i \\ \dot{y}_i = v_i \sin\theta_i \\ \dot{\theta}_i = \omega_i \\ \dot{v}_i = u_i \end{cases} \tag{2.5}$$

If a rigid formation is assigned for N agents, the desired position of the i^{th} agent in **VS** is specified by α_i and d_i in Eq.(2.3). One can establish a controller which

stabilizes these errors using a suitable Lyapunov function. Let us define $s_{i,l}$ and $s_{i,\theta}$ as the following;

$$\begin{aligned} s_{i,l} =& \left(\frac{\gamma_{i,l} + \lambda_{i,l}}{\gamma_{i,l}\lambda_{i,l}} + \frac{1 + \gamma_{i,l}\lambda_{i,l}}{(\gamma_{i,l} + \lambda_{i,l})} \right) e_{i,l}^2 + \frac{2}{\gamma_{i,l}\lambda_{i,l}} e_{i,l}\dot{e}_{i,l} \\ &+ \left(\frac{1 + \gamma_{i,l}\lambda_{i,l}}{\gamma_{i,l}\lambda_{i,l}(\gamma_{i,l} + \lambda_{i,l})} \right) \dot{e}_{i,l}^2 \\ s_{i,\theta} =& \left(\frac{\gamma_{i,\theta} + \lambda_{i,\theta}}{\gamma_{i,\theta}\lambda_{i,\theta}} + \frac{1 + \gamma_{i,\theta}\lambda_{i,\theta}}{(\gamma_{i,\theta} + \lambda_{i,\theta})} \right) e_{i,\theta}^2 + \frac{2}{\gamma_{i,\theta}\lambda_{i,\theta}} e_{i,\theta}\dot{e}_{i,\theta} \\ &+ \left(\frac{1 + \gamma_{i,\theta}\lambda_{i,\theta}}{\gamma_{i,\theta}\lambda_{i,\theta}(\gamma_{i,\theta} + \lambda_{i,\theta})} \right) \dot{e}_{i,\theta}^2 \end{aligned} \tag{2.6}$$

where $\lambda_{i,l} > 0$, $\gamma_{i,l} > 0$, $\lambda_{i,\theta} > 0$, and $\gamma_{i,\theta} > 0$. Consider the following Lyapunov function candidate.

$$\mathcal{V} = \frac{1}{2} \sum_{i}^{N} (s_{i,l} + s_{i,\theta}) \tag{2.7}$$

If $\mathbf{u}_i$ satisfies $\ddot{e}_{i,l} = -(\gamma_{i,l} + \lambda_{i,l})\dot{e}_{i,l}^2 - \gamma_{i,l}\lambda_{i,l}e_{i,l}$ and $\ddot{e}_{i,\theta} = -(\gamma_{i,\theta} + \lambda_{i,\theta})\dot{e}_{i,\theta}^2 - \gamma_{i,\theta}\lambda_{i,\theta}e_{i,\theta}$, the derivative of Lyapunov function $\dot{\mathcal{V}}$ will be $-\sum_{i}^{N}(\dot{e}_{i,l}^2 + e_{i,l}^2 + \dot{e}_{i,\theta}^2 + e_{i,\theta}^2) \leq 0$. Since $(e_{i,l}, \dot{e}_{i,l}, e_{i,\theta}, \dot{e}_{i,\theta}) = (0, 0, 0, 0)$ is the largest invariant set in $\{\mathbf{x} | \dot{\mathcal{V}}(\mathbf{x}) = 0\}$, the errors will be asymptotically stabilized by the LaSalle's theorem. The control inputs appear in the second derivatives of the errors, and each control law for the actual agents can be calculated by solving two linear equations as follows;

$$\begin{aligned} \ddot{e}_{i,l} &= D_i + B_i u_i + C_i \omega_i \\ \ddot{e}_{i,\theta} &= DD_i + BB_i u_i + CC_i \omega_i \end{aligned} \tag{2.8}$$

where

$$
\begin{aligned}
D_i &= 2\dot{\tilde{x}}_i^2 + 2\dot{\tilde{y}}_i^2 - 2\tilde{x}_i\ddot{x}_{v1} - 2\tilde{y}_i\ddot{y}_{v1},\\
B_i &= 2\tilde{x}_i\cos\theta_i + 2\tilde{y}_i\sin\theta_i,\\
C_i &= -2\tilde{x}_i\dot{y}_i + 2\tilde{y}_i\dot{x}_i,\\
DD_i &= -\frac{\tilde{x}_i\ddot{y}_{v1} - \ddot{x}_{v1}\tilde{y}_i}{\tilde{x}_i^2+\tilde{y}_i^2} - \frac{\tilde{x}_{v2}\dddot{y}_{v2} - \dddot{x}_{v2}\tilde{y}_{v2}}{\tilde{x}_{v2}^2+\tilde{y}_{v2}^2} - \frac{(\tilde{x}_i\dot{\tilde{y}}_i - \dot{\tilde{x}}_i\tilde{y}_i)(2\tilde{x}_i\dot{\tilde{x}}_i + 2\tilde{y}_i\dot{\tilde{y}}_i)}{(\tilde{x}_i^2+\tilde{y}_i^2)^2}\\
&\quad + \frac{(\tilde{x}_{v2}\dot{\tilde{y}}_{v2} - \dot{\tilde{x}}_{v2}\tilde{y}_{v2})(2\tilde{x}_{v2}\dot{\tilde{x}}_{v2} + 2\tilde{y}_{v2}\dot{\tilde{y}}_{v2})}{(\tilde{x}_{v2}^2+\tilde{y}_{v2}^2)^2},\\
BB_i &= \frac{\tilde{x}_i\cos\theta_i - \tilde{y}_i\sin\theta_i}{\tilde{x}_i^2+\tilde{y}_i^2},\\
CC_i &= \frac{\tilde{x}_i\dot{x}_i + \tilde{y}_i\dot{y}_i}{\tilde{x}_i^2+\tilde{y}_i^2},\\
\tilde{x}_i &= x_i - x_{v1}, \quad \tilde{y}_i = y_i - y_{v1}, \quad \tilde{x}_{v2} = x_{v2} - x_{v1}, \quad \tilde{y}_{v2} = y_{v2} - y_{v1}.
\end{aligned}
$$

Therefore, the control law $\mathbf{u}_i$ is determined as follows;

$$
\begin{bmatrix} C_i & B_i \\ CC_i & BB_i \end{bmatrix} \mathbf{u}_i = \begin{bmatrix} F_i \\ G_i \end{bmatrix} \tag{2.9}
$$

where

$$
\begin{aligned}
F_i &= -\lambda_{i,l}\dot{e}_{i,l} - \gamma_{i,l}(\dot{e}_{i,l} + \lambda_{i,l}e_{i,l}) - A_i\\
G_i &= -\lambda_{i,\theta}\dot{e}_{i,\theta} - \gamma_{i,\theta}(\dot{e}_{i,\theta} + \lambda_{i,\theta}e_{i,\theta}) - AA_i.
\end{aligned}
$$

The paths of the two virtual leaders $\mathbf{VL}_1$, $\mathbf{VL}_2$ coordinates the motion of the VS, and the control law $\mathbf{u}_i$ forces the agents to remain in formation.

2. 3D Dynamic Model of Agent

Now we discuss designing a controller which stabilizes the formation errors in $\mathcal{R}^3$. Simple kinematic model for agent in $\mathcal{R}^3$ can be represented by Eq.(2.1) where $\mathbf{z}_i = [x_i, y_i, z_i, \theta_i, \alpha_i, v_i]^T$, $f_i(\mathbf{z}_i) = [v_i\cos\theta_i\cos\alpha_i, v_i\sin\theta_i\cos\alpha_i, v_i\sin\alpha_i, 0, 0, 0]^T$, $g_i(\mathbf{z}_i) =$

$[g_{i,1}, g_{i,2}, g_{i,3}]$, $g_{i,1} = [0,0,0,1,0,0]^T$,$g_{i,2} = [0,0,0,0,1,0]^T$,$g_{i,3} = [0,0,0,0,0,1]^T$, $h_i = [h_{i,1}, h_{i,2}, h_{i,3}]^T = [x_i - x_i^*, y_i - y_i^*, z_i - z_i^*]^T = [\overline{x}_i, \overline{y}_i, \overline{z}_i]^T$, and $\mathbf{u}_i = [\omega_i, \tau_i, u_i]^T$. Namely, the following form represents the dynamics of each agent.

$$\begin{cases} \dot{x}_i = v_i \cos\theta_i \cos\phi_i \\ \dot{y}_i = v_i \sin\theta_i \cos\phi_i \\ \dot{z}_i = v_i \sin\alpha_i \\ \dot{\theta}_i = \omega_i \\ \dot{\phi}_i = \tau_i \\ \dot{v}_i = u_i \end{cases} \tag{2.10}$$

Formation Constraints can be defined by $Q_i = [r_i^*]_I - [\mathbf{b}_i]_I = 0$ and formation errors are represented by $\mathbf{E}_i = [r_i]_I - [r_i^*]_I$. Let us define the error vector for the i^{th} subsystem in the following form;

$$\mathbf{E}_i = \begin{bmatrix} \overline{x}_i \\ \overline{y}_i \\ \overline{z}_i \end{bmatrix} = \begin{bmatrix} x_i - x_i^* \\ y_i - y_i^* \\ z_i - z_i^* \end{bmatrix} \tag{2.11}$$

Let $\mathbf{y}_i$ be $\mathbf{E}_i$, and let us define $\gamma_{i,j}$ to be the relative degree for the j^{th} output of the i^{th} subsystem. We can see that all the relative degrees of outputs are 2 in Eq.(2.12). Namely, $\gamma_{i,1} = 2$, $\gamma_{i,2} = 2$, and $\gamma_{i,3} = 2$. The total relative degree γ_i is $\gamma_{i,1} + \gamma_{i,2} + \gamma_{i,3} =$

$6 = n$. Therefore no internal dynamics appear in the normal form.

$$\begin{aligned}
\dot{\bar{x}}_i &= L_{f_i}h_{i,1} + L_{g_{i,1}}h_{i,1}\omega_i + L_{g_{i,2}}h_{i,1}\tau_i + L_{g_{i,3}}h_{i,1}u_i = v_i\cos\theta_i\cos\phi_i - \dot{x}_i^* \\
\ddot{\bar{x}}_i &= L_{f_i}^2h_{i,1} + L_{g_{i,1}}L_{f_i}h_{i,1}\omega_i + L_{g_{i,2}}L_{f_i}h_{i,1}\tau_i + L_{g_{i,3}}L_{f_i}h_{i,1}u_i \\
&= -\ddot{x}_i^* - v_i\sin\theta_i\cos\phi_i\omega_i - v_i\cos\theta_i\sin\phi_i\tau_i + \cos\theta_i\cos\phi_i u_i \\
\dot{\bar{y}}_i &= L_{f_i}h_{i,2} + L_{g_{i,1}}h_{i,2}\omega_i + L_{g_{i,2}}h_{i,2}\tau_i + L_{g_{i,3}}h_{i,2}u_i = v_i\sin\theta_i\cos\phi_i - \dot{y}_i^* \\
\ddot{\bar{y}}_i &= L_{f_i}^2h_{i,2} + L_{g_{i,1}}L_{f_i}h_{i,2}\omega_i + L_{g_{i,2}}L_{f_i}h_{i,2}\tau_i + L_{g_{i,3}}L_{f_i}h_{i,2}u_i \\
&= -\ddot{y}_i^* + v_i\cos\theta_i\cos\phi_i\omega_i - v_i\sin\theta_i\sin\phi_i\tau_i + \sin\theta_i\cos\phi_i u_i \\
\dot{\bar{z}}_i &= L_{f_i}h_{i,3} + L_{g_{i,1}}h_{i,3}\omega_i + L_{g_{i,2}}h_{i,3}\tau_i + L_{g_{i,3}}h_{i,3}u_i = -v_i\sin\phi_i - \dot{z}_i^* \\
\ddot{\bar{z}}_i &= L_{f_i}^2h_{i,3} + L_{g_{i,1}}L_{f_i}h_{i,3}\omega_i + L_{g_{i,2}}L_{f_i}h_{i,3}\tau_i + L_{g_{i,3}}L_{f_i}h_{i,3}u_i \\
&= -\ddot{z}_i^* + v_i\cos\phi_i\tau_i - \sin\phi_i u_i
\end{aligned} \tag{2.12}$$

The error dynamics of the i^{th} subsystem can be expressed in the following form.

$$\begin{aligned}
\ddot{\mathbf{E}}_i &= -\ddot{\mathbf{r}}_i^* + \mathbf{A}_i(\mathbf{z}_i)\mathbf{u}_i \\
\ddot{\mathbf{E}}_i &= \nu_i \\
\mathbf{u}_i &= \mathbf{A}_i(\mathbf{z}_i)^{-1}(\nu_i + \ddot{\mathbf{r}}_i^*)
\end{aligned} \tag{2.13}$$

where

$$\begin{aligned}
\mathbf{A}_i(\mathbf{z}_i) &= \begin{bmatrix} L_{g_{i,1}}L_{f_i}h_{i,1} & L_{g_{i,2}}L_{f_i}h_{i,1} & L_{g_{i,3}}L_{f_i}h_{i,1} \\ L_{g_{i,1}}L_{f_i}h_{i,2} & L_{g_{i,2}}L_{f_i}h_{i,2} & L_{g_{i,3}}L_{f_i}h_{i,2} \\ L_{g_{i,1}}L_{f_i}h_{i,3} & L_{g_{i,2}}L_{f_i}h_{i,3} & L_{g_{i,3}}L_{f_i}h_{i,3} \end{bmatrix} \\
&= \begin{bmatrix} -v_i\sin\theta_i\cos\phi_i & -v_i\cos\theta_i\sin\phi_i & \cos\theta_i\cos\phi_i \\ v_i\cos\theta_i\cos\phi_i & -v_i\sin\theta_i\sin\phi_i & \sin\theta_i\cos\phi_i \\ 0 & v_i\cos\phi_i & -\sin\phi_i \end{bmatrix} \\
\ddot{\mathbf{r}}_i^* &= \begin{bmatrix} \ddot{x}_i^* & \ddot{y}_i^* & \ddot{z}_i^* \end{bmatrix}^T
\end{aligned}$$

Suppose ν_i satisfies the following form;

$$\nu_i = \mathbf{J}_i\dot{\mathbf{E}}_i + \mathbf{K}_i(\dot{\mathbf{E}}_i - \mathbf{J}_i\mathbf{E}_i) \tag{2.14}$$

where $\mathbf{J}_i$ and $\mathbf{K}_i$ are Hurwitz. Let us define the error vector for the composite system as $\mathbf{E} = [\mathbf{E}_1^T, \dot{\mathbf{E}}_1^T, \mathbf{E}_2^T, \dot{\mathbf{E}}_2^T, \cdots, \mathbf{E}_n^T, \dot{\mathbf{E}}_n^T]^T \in \mathcal{R}^{2Nn}$. Lyapunov function candidate can be defined by $\mathcal{V}(\mathbf{E}) = \sum_i^N \chi_i^T\mathbf{P}_i\chi_i$ where $\chi_i = [\mathbf{E}_i^T, \dot{\mathbf{E}}_i^T]^T$ and $\mathbf{P}_i$ is a symmetric positive definite matrix in $\mathcal{R}^{2n\times 2n}$. By Eq.(2.13)and Eq.(2.14), χ_i should satisfy the following condition.

$$\dot{\chi}_i = \begin{bmatrix} 0 & \mathbf{I} \\ -\mathbf{K}_i\mathbf{J}_i & \mathbf{J}_i + \mathbf{K}_i \end{bmatrix} \chi_i = \mathbf{H}_i\chi_i \tag{2.15}$$

the derivative of the Lyapunov function is $\dot{\mathcal{V}}(\mathbf{E}) = \sum_i^N \chi_i^T(\mathbf{H}_i^T\mathbf{P}_i + \mathbf{P}_i\mathbf{H}_i)\chi_i$. Suppose $\mathbf{P}_i$ is the solution of $\mathbf{H}_i^T\mathbf{P}_i^T + \mathbf{P}_i\mathbf{H}_i = -\mathbf{I}$. Then, $\dot{\mathcal{V}}(\mathbf{E}) = -\sum_i^N \chi_i^T\chi_i = -\sum_i^N \|\chi_i\|^2 = -\|\mathbf{E}\|^2 \leq 0$. Since the Lyapunov function satisfies the following inequalities

$$\min\{\text{eig}(\mathbf{P}_i)\}\|\mathbf{E}\|^2 \leq \mathcal{V}(\mathbf{E}) \leq \max\{\text{eig}(\mathbf{P}_i)\}\|\mathbf{E}\|^2$$
$$\frac{\partial\mathcal{V}}{\partial t} + \frac{\partial\mathcal{V}}{\partial\mathbf{E}}\dot{\mathbf{E}} \leq -\|\mathbf{E}\|^2$$

the formation errors are stabilized exponentially and globally which follows from theorem 4.10 in [27]. Therefore, the controller $\mathbf{u}_i$ is represented by the following.

$$\mathbf{u}_i = \mathbf{A}_i(\mathbf{z}_i)^{-1}\Big\{(\mathbf{J}_i + \mathbf{K}_i)\dot{\mathbf{E}}_i - \mathbf{K}_i\mathbf{J}_i\mathbf{E}_i + \ddot{\mathbf{r}}_i^*\Big\} \tag{2.16}$$

F. Simulation Results

Figure 5 depicts a scenario where six agents maneuver to construct a hexagonal formation starting from arbitrary initial conditions by employing the controllers $\mathbf{u}_i$ proposed in Eq.(2.9). The initial conditions for actual agents and the virtual agents

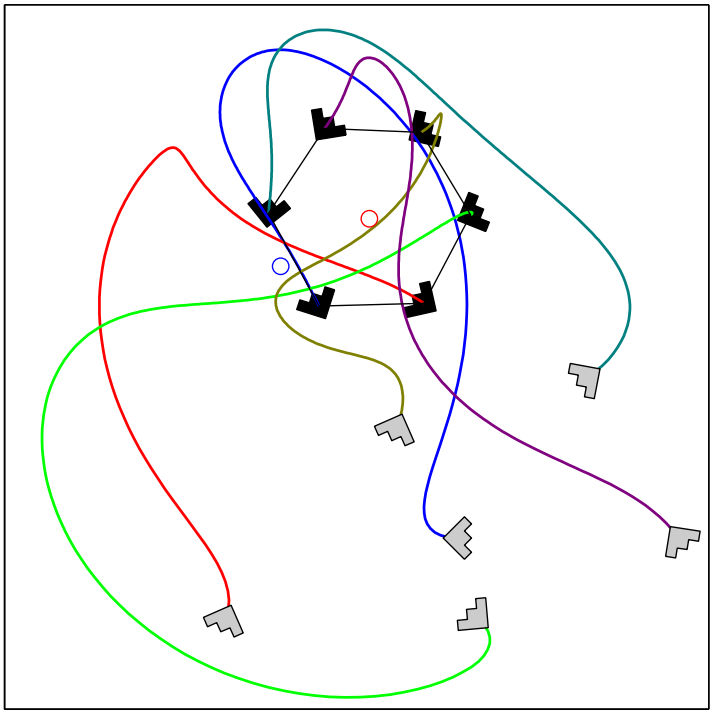

Fig. 5. Forming hexagonal formation. Gray shows initial configuration of agents and black shows accomplished formation

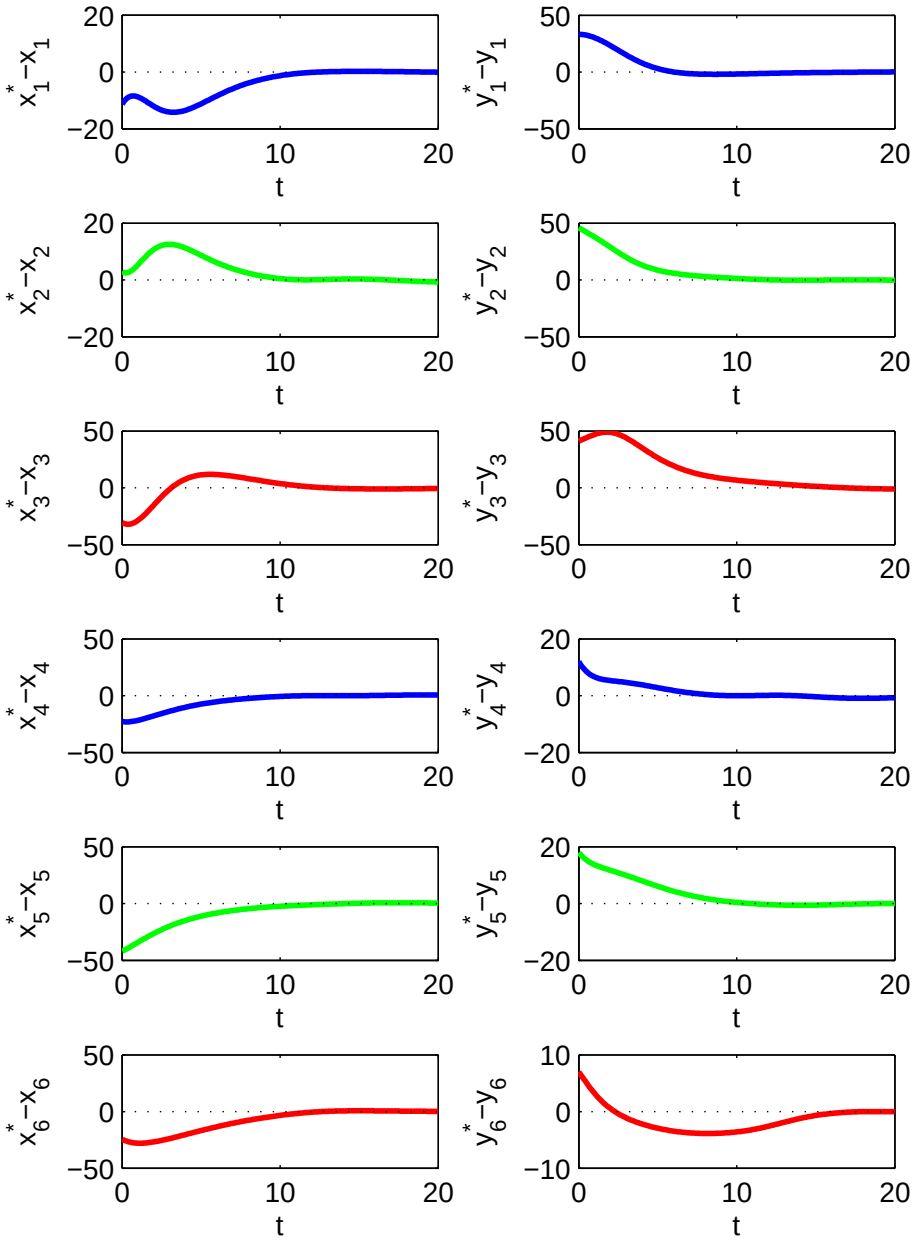

Fig. 6. All errors are stabilized exponentially by proposed controllers

used in simulation are given by Table I. The desired hexagonal rigid formation was specified by the values in Table II. The hexagonal rigid formation was steered by

Table I. Initial Conditions

States	$i=1$	$i=2$	$i=3$	$i=4$	$i=5$	$i=6$	$i=v1$	$i=v2$
$x_i(m)$	10	-13	12	4	32	23	-10	0
$y_i(m)$	-48	-56	-56	-37	-48	-32	-20	-20
$\theta_i(rad)$	$-\pi$	1.2	-0.7	1.2	2.2	0.6	$\frac{\pi}{2}$	$\frac{\pi}{2}$
$v_i(m/sec)$	10	10	10	10	10	10	1	2

Table II. Specification of Formation

	$i=1$	$i=2$	$i=3$	$i=4$	$i=5$	$i=6$
$d_i(m)$	10	10	10	10	10	10
$\alpha_i(rad)$	$\frac{\pi}{6}$	$\frac{\pi}{2}$	$\frac{5\pi}{6}$	$-\frac{5\pi}{6}$	$-\frac{\pi}{2}$	$-\frac{\pi}{6}$

two virtual agents $\mathbf{VL}_1$ and $\mathbf{VL}_2$ which were shown by red and blue circles in Fig.5. Since these two virtual agents maintain constant distance d_v, the following equation is always true.

$$\|[\mathbf{r}_{v2} - \mathbf{r}_{v1}]_I\| = d_v \tag{2.17}$$

In this simulation, models of virtual agents were taken to be the same as that of the actual agents. However, it is not necessary that the models of virtual agents be the same as that of actual agents. The first virtual agent was located at O_B, and the second virtual agent at $[d_v, 0]$ in the frame B. The controls for the first virtual agent were chosen to be $u_{v1} = 0$, $\omega_{v1} = -0.2\sin(\frac{t}{10})$, and the control for the second virtual agent was chosen to be $u_{v2} = 0$. However, these values can be chosen arbitrarily. The angular velocity of the second virtual agent was determined

from Eq.(2.17). Also, Fig.6 shows that all errors are stabilized exponentially by the controllers $\mathbf{u}_i$ in Eq.(2.9). The i^{th} row in Fig.6 shows the errors between $[\mathbf{r}_i]_I$ and $[\mathbf{r}_i^*]_I$. The convergence rate was determined by $\lambda_{i,l}$, $\lambda_{i,\theta}$, $\gamma_{i,l}$, and $\gamma_{i,l}$, and these values were chosen to be $\lambda_{i,l} = 0.5$, $\lambda_{i,\theta} = 0.5$, $\gamma_{i,l} = 0.4$, and $\gamma_{i,l} = 0.4$. Note that the matrix $P = \begin{bmatrix} C_i & B_i \\ CC_i & BB_i \end{bmatrix}$ can be singular when the i^{th} agent coincides with the virtual leaders or when the i^{th} agent is stationary. While the former case can be avoided by choosing $\alpha_i \neq 0,\ d_i > 0$, in the latter case, no smooth time-invariant control law can stabilize the error. This well known result is found in [29].

CHAPTER III

PRACTICAL CONTROLLER

A. Singularity

As was shown in the previous chapters, the designed controller will fail when $v_i = 0$. Even if $v_i \neq 0$, there exits a small value ε such that an ill-condition in matrix inversion will occur for $v_i \leq \varepsilon$. Computation of the previous designed controller become a challenge as each agent approaches the desired position in the stationary rigid formation. This problem is similar to the stabilization problem of a unicycle system in cartesian coordinates. The theorem in [29] shows that the stabilization for the unicycle model in cartesian coordinates can not be solved. However, if the state itself is not defined at the origin of the frame, the theorem in [29] will not be an obstruction to stabilization any more. By a nonlinear coordinate transformation, a unicycle model is stabilizable [30]. Mapping from the cartesian coordinates to the polar coordinates can be one such nonlinear coordinate transformations. The representation of unicycle model in polar coordinates is introduced in [31, 32]. The relationship between a representation by cartesian coordinates and a representation by polar coordinates is shown in Fig.7.

$$\begin{cases} \dot{\rho} = -v\cos\sigma \\ \dot{\varphi} = \dfrac{v}{\rho}\sin\sigma \\ \dot{\sigma} = \dfrac{v}{\rho}\sin\sigma - \omega \end{cases} \tag{3.1}$$

Equation (3.1) shows the unicycle model in polar coordinates where

$$\rho = \sqrt{x^2 + y^2} \qquad \varphi = \tan^{-1}\left(\frac{-y}{-x}\right) \qquad \sigma = \varphi - \theta \tag{3.2}$$

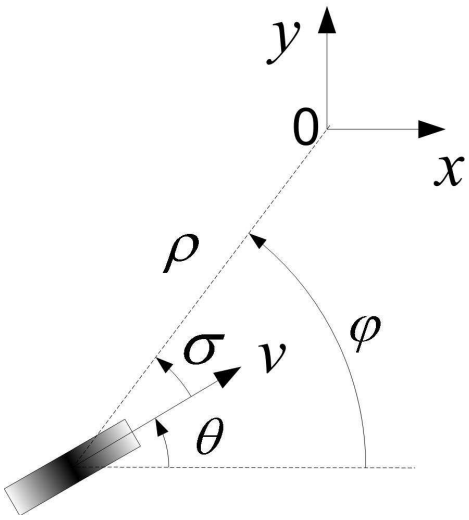

Fig. 7. The representation of unicycle model in polar coordinates

This model can be represented by $\dot{\mathbf{z}} = f(\mathbf{z}, \mathbf{u})$ where $\mathbf{z}$ is the state vector, $\mathbf{u}$ is the control input vector, and the domain of the function f is $D = \mathcal{R}^2 - \{0\}$. To study the stability of the origin we define a Lyapunov function $\mathcal{V}_p$ as

$$\mathcal{V}_p = \frac{1}{2}\rho^2 + \frac{1}{2}\varphi^2 + \frac{1}{2}\sigma^2 > 0 \quad \text{in} \quad D.$$

The derivative of the Lyapunov function candidate $\mathcal{V}_p$ along the trajectories of Eq.(3.1) is

$$\begin{aligned} \dot{\mathcal{V}}_p &= \rho\dot{\rho} + \varphi\dot{\varphi} + \sigma\dot{\sigma} \\ &= -v\rho\cos\sigma + v\frac{(\varphi+\sigma)}{\rho}\sin\sigma - \sigma\omega. \end{aligned}$$

Let us choose the controls v and ω as the following;

$$\begin{aligned} v &= M\tanh\left(\frac{k_1\rho}{\cos\sigma}\right) \\ \omega &= (\varphi+\sigma)M\tanh\left(\frac{k_1\rho}{\cos\sigma}\right)\frac{\sin\sigma}{\rho\sigma} + k_2 M\tanh\sigma \end{aligned} \tag{3.3}$$

where M, k_1, and k_2 are positive constants. Since $0 < \frac{\tanh(\zeta x)}{x} \leq \zeta$ holds for $x \in \mathcal{R}$, The derivative of $\mathcal{V}_p$ is always negative definite in the domain D.

$$\dot{\mathcal{V}}_p \leq -Mk_1\rho^2 \leq 0 \tag{3.4}$$

In order to apply this controllers to the system (2.10), we need the time derivative of the velocity.

$$\begin{aligned}
\dot{v} &= Mk_1\mathrm{sech}^2\left(\frac{k_1\rho}{\cos\sigma}\right)\left\{\frac{\dot{\rho}\cos\sigma + \rho\dot{\sigma}\sigma}{\cos^2\sigma}\right\} \\
&= Mk_1\mathrm{sech}^2\left(\frac{k_1\rho}{\cos\sigma}\right)\left\{\frac{-v\cos^2\sigma + v\sin^2\sigma - \rho\omega\sin\sigma}{\cos^2\sigma}\right\} \\
&= -Mk_1\mathrm{sech}^2\left(\frac{k_1\rho}{\cos\sigma}\right)\left\{v + v\frac{\varphi}{\sigma}\tan^2\sigma + k_2M\rho\tanh\sigma\tan\sigma\sin\sigma\right\}
\end{aligned}$$

Therefore, the controllers for the i^{th} agent whose $|v_i|$ is smaller than ε can be chosen in the following form.

$$\begin{cases}
\omega_i = (\varphi_i + \sigma_i)v_i\dfrac{\sin\sigma_i}{\rho\sigma - i} + k_2M\tanh\sigma_i \\
u_i = -Mk_1\mathrm{sech}^2\left(\dfrac{k_1\rho_i}{\cos\sigma_i}\right)\left\{v_i + v_i\dfrac{\varphi}{\sigma_i}\tan^2\sigma_i + k_2M\rho_i\tanh\sigma_i\tan\sigma_i\sin\sigma_i\right\}
\end{cases} \tag{3.5}$$

where

$$\rho_i = \sqrt{x_i^2 + y_i^2}, \quad \varphi_i = \tan^{-1}\left(\frac{-y_i}{-x_i}\right), \quad \text{and} \quad \sigma_i = \varphi_i - \theta_i \quad .$$

B. Robust Stability by Lyapunov Redesign

If there are uncertain terms in the dynamics of agents, the controller which was designed for the nominal plant can not guarantee the stability of rigid formation. We assume that the system dynamics of the i^th agent can be represented by the

followings;

$$\begin{aligned}\dot{\mathbf{z}}_i &= f_i(t, \mathbf{z}_i) + g_i(t, \mathbf{z}_i)[\mathbf{u}_i + \delta_i(t, \mathbf{z}_i, \mathbf{u}_i)] \\ \mathbf{r}_i &= h_i(\mathbf{z}_i)\end{aligned} \tag{3.6}$$

The function f_i and g_i are known precisely, while the function δ is an unknown function that lumps together uncertain terms due to model simplification, parameter uncertainty, and so on. Let the previously designed controller for nominal plant be $\mathbf{u}_i^*$. Since this controller stabilizes a formation error exponentially, the Lyapunov function $\mathcal{V}_i(\mathbf{E_i}) = \mathbf{E}_i^T \mathbf{P}_i \mathbf{E}_i$ along the trajectory of the nominal plant of the i^{th} subsystem satisfies the following condition.

$$\dot{\mathcal{V}}_i = \frac{\partial \mathcal{V}_i}{\partial t} + \frac{\partial \mathcal{V}_i}{\partial \mathbf{E}_i}(f_i + g_i \mathbf{u}_i^*) + \frac{\partial \mathcal{V}_i}{\partial \mathbf{E}_i} g_i(\Delta \mathbf{u}_i + \delta_i) \leq -\|\mathbf{E}_i\|^2 + \frac{\partial \mathcal{V}_i}{\partial \mathbf{E}_i} g_i(\Delta \mathbf{u}_i + \delta_i) \tag{3.7}$$

Set $\mu_i = \frac{\partial \mathcal{V}_i}{\partial \mathbf{E}_i} g_i$ and rewrite the last inequality as

$$\dot{\mathcal{V}}_i \leq -\|\mathbf{E}_i\|^2 + \mu_i^T \Delta \mathbf{u}_i + \mu_i^T \delta_i \tag{3.8}$$

Let us assume that the uncertain term δ_i satisfies the following condition.

$$\|\delta_i(t, \mathbf{E}_i, \mathbf{u}_i^* + \Delta \mathbf{u}_i)\| \leq \rho_i(t, \mathbf{E}_i) + k_i \|\Delta \mathbf{u}_i\|, \qquad 0 < k_i < 1 \tag{3.9}$$

The following inequality can be driven from the right hand side of inequality (3.8) by the assumed inequality (3.9).

$$\mu_i^T \Delta \mathbf{u}_i + \mu_i^T \delta_i \leq \mu_i^T \Delta \mathbf{u}_i + \|\mu_i\| \|\delta_i\| \leq \mu_i^T \Delta \mathbf{u}_i + \|\mu_i\|(\rho_i(t, \mathbf{E}_i) + k_i \|\Delta \mathbf{u}_i\|) \tag{3.10}$$

Take the following form for $\Delta \mathbf{u}_i$.

$$\Delta \mathbf{u}_i = -\frac{\rho_i}{1 - k_i} \frac{\mu_i}{\|\mu_i\|} \tag{3.11}$$

Then, the right hand side of inequality (3.8) will be canceled.

$$\mu_i^T \Delta \mathbf{u}_i + \mu_i^T \delta_i \leq -\frac{\rho_i}{1-k_i}\|\mu_i\| + \rho_i\|\mu_i\| + \frac{\rho_i k_i}{1-k_i}\|\mu_i\| = 0 \tag{3.12}$$

Therefore $\dot{\mathcal{V}}_i(\mathbf{E}_i) \leq -\|\mathbf{E}_i\|^2$, and the i^{th} subsystem with uncertain term δ_i can be stabilized by the controller $\mathbf{u}_i = \mathbf{u}_i^* - \frac{\rho_i}{1-k_i}\frac{\mu_i}{\|\mu_i\|}$.

C. Formation Guidance

Now we consider another practical issue in formation control. In the previous chapter(Ch.II), we focussed on the generation of a formation. The proposed controller only guarantees that all agents maintain specified distances between agents. But there is no formation guidance scheme. In what follows we consider a rendezvous problem. In order to drive a group of agents to assemble at a common location, we need a scheme for guiding a generated formation. Here, we do not consider control bounds for agents. A feasible solution with control bounds can be found in [21]. The proposed scheme in the previous chapter(Ch.II) introduced virtual agents to construct a rigid formation. We can utilize these virtual agents to guide a rigid formation. A rigid formation is assumed a **VS** which is composed of N agents and 2 virtual agents in $\mathcal{R}^2$. If we want the rigid formation to move with a linear velocity v_{VS} and an angular velocity $\dot{\Theta}$ by controlling virtual agents, we should know the relationship between them. Let the frame B be fixed on the **VS** and its origin be located at O_B. $\mathbf{r}_{v1}$, $\mathbf{r}_{v2}$, and $\mathbf{r}_{VS}$ denote the position vectors of the first virtual agent, the second virtual agent, and the origin of the frame B with respect to the inertial frame, respectively. The coordinates of the position vectors is represented by the following:

$$[\mathbf{r}_{VS}]_I = \begin{bmatrix} x_{VS} \\ y_{VS} \end{bmatrix} \qquad [\mathbf{r}_{v1}]_I = \begin{bmatrix} x_{v1} \\ y_{v1} \end{bmatrix} \qquad [\mathbf{r}_{v2}]_I = \begin{bmatrix} x_{v2} \\ y_{v2} \end{bmatrix} \tag{3.13}$$

The **VS** as well as virtual agents are modeled as unicycles and are given by

$$\begin{bmatrix} \dot{x}_{VS} \\ \dot{y}_{VS} \\ \dot{\Theta} \end{bmatrix} = \begin{bmatrix} v_{VS}\cos\Theta \\ v_{VS}\sin\Theta \\ \Omega \end{bmatrix}, \quad \begin{bmatrix} \dot{x}_{v1} \\ \dot{y}_{v1} \\ \dot{\theta}_{v1} \end{bmatrix} = \begin{bmatrix} v_{v1}\cos\theta_{v1} \\ v_{v1}\sin\theta_{v1} \\ \omega_{v1} \end{bmatrix}, \quad \begin{bmatrix} \dot{x}_{v2} \\ \dot{y}_{v2} \\ \dot{\theta}_{v2} \end{bmatrix} = \begin{bmatrix} v_{v2}\cos\theta_{v1} \\ v_{v2}\sin\theta_{v1} \\ \omega_{v2} \end{bmatrix}. \quad (3.14)$$

The locations of virtual agents can be chosen freely on the **VS** unless they coincide. The main reason of locating one virtual agent at the mass center of **VS** is that the origin can move in holonomic way even if all agents have nonholonomic dynamics. In other words, a rigid formation constructed by nonholonomic agents can follow trajectories of a target whose dynamics are holonomic. To utilize this advantage, the position of the first virtual agent is chosen to be the origin of frame B, and the second virtual agent is denoted by the position vector $\mathbf{d}_{v2}$ with respect to frame B for simplicity. Therefore the following conditions hold.

$$\begin{aligned} \mathbf{r}_{v1} &= \mathbf{r}_{VS} \\ \mathbf{r}_{v2} &= \mathbf{r}_{v1} + \mathbf{d}_{v2} \end{aligned} \quad (3.15)$$

where $[\mathbf{d}_{v2}]_B = [d_{v2}, 0]^T$. The velocities can be obtained from differentiation of Eq.(3.15) to get

$$\begin{aligned} \left[\dot{\mathbf{r}}_{v1}\right]_I &= \left[\dot{\mathbf{r}}_{VS}\right]_I \\ \left[\dot{\mathbf{r}}_{v2}\right]_I &= \left[\dot{\mathbf{r}}_{v1}\right]_I + \dot{\mathbf{R}}(\Theta)\left[\mathbf{d}_{v2}\right]_B \end{aligned} \quad . \quad (3.16)$$

If we want the **VS** to move with $v_{VS} = U$ and $\dot{\Theta} = \Omega$, v_{v1}, v_{v2}, ω_{v1}, and ω_{v2} should be chosen corresponding to U and Ω. The values of control inputs of virtual agents

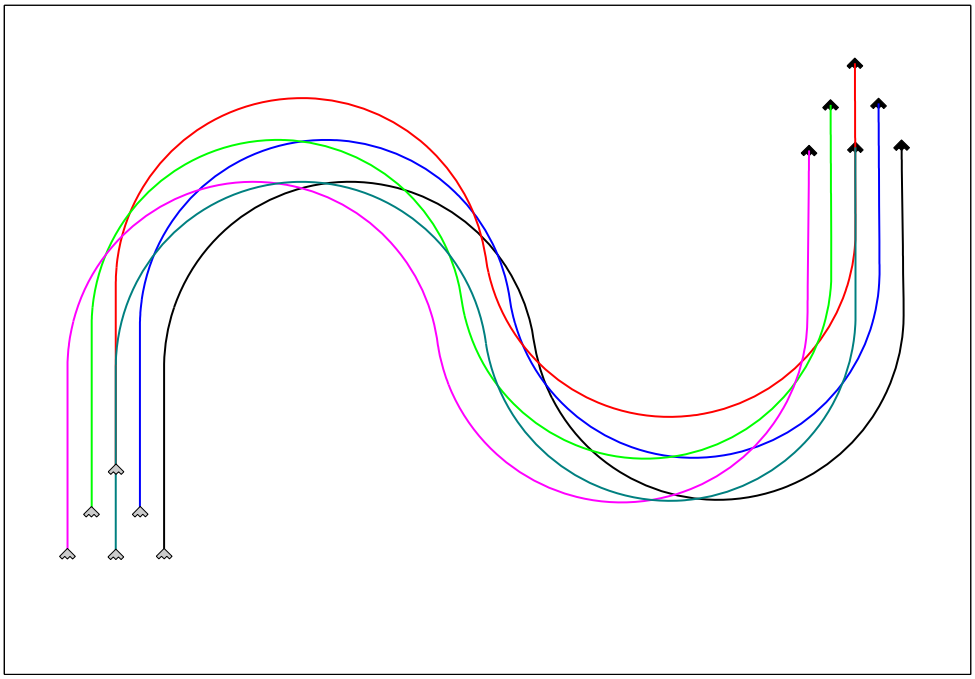

Fig. 8. Translational motion of a rigid triangular formation

can be obtained from Eq.(3.16) and Eq.(3.14).

$$\begin{aligned} v_{v1} &= v_{VS}\cos(\Theta - \theta_{v1}) \\ \omega_{v1} &= \frac{\dot{v}_{VS}\sin(\Theta - \theta_{v1}) + v_{VS}\Omega\cos(\Theta - \theta_{v1})}{v_{v1}} \\ v_{v2} &= \sqrt{v_{VS}^2 + \Omega^2 d_{v2}^2} \\ \omega_{v2} &= \frac{\Omega v_{VS}^2 + \dot{\Omega} v_{VS} d_{v2} - \dot{v}_{VS}\Omega d_{v2} + \Omega^3 d_{v2}^2}{v_{VS}^2 + \Omega^2 d_{v2}^2} \end{aligned} \tag{3.17}$$

Figure 8 shows the translational motion of a rigid triangular formation composed of 6 agents where $\Omega = 0$. This simulation shows that a rigid formation can move along a curvilinear path without rotation. Also, Fig.9 shows the rotational motion of rigid triangular formation along the same path as in Fig.9 where $\Omega = 0.1$rad/sec. As seen from Fig.8 and Fig.9, the orientation of a rigid formation can be independent of a path curvature. This is one of the main differences between leader-follower schemes

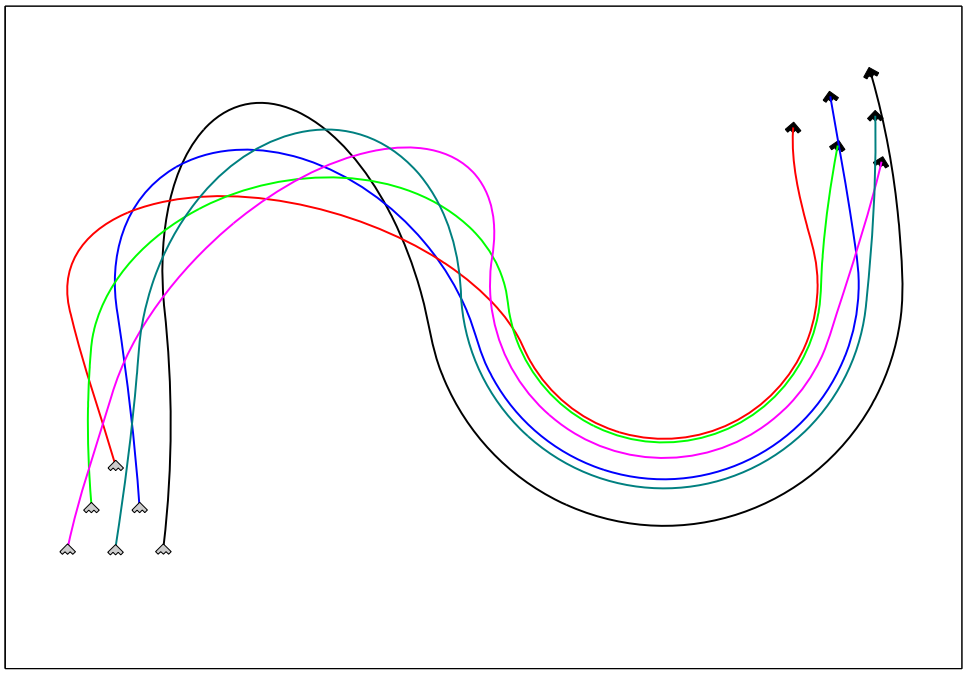

Fig. 9. Rotational motion of a rigid triangular formation

and the scheme proposed in this dissertation. A rigid formation constructed by the leader-follower approach does not have freedom of its orientation from path curvature.

D. Transformation between Rigid Formations

Another issue in applying formation generation scheme to formation control problem is shape change of a formation. To meet group objectives, formation shape may have to be changed. Such objectives could include obstacle avoidance or saving fuel of agents. Formation reconfiguration can be thought of as changing a shape of a rigid formation. A shape of rigid formation is represented by desired positions of agents in the frame B which is fixed on the **VS**. Therefore, shape change can be achieved by redefining the desired positions of agents in frame B. Errors will occur when $[\mathbf{r}_i^*]_B$ are redefined and the formation is in transition from one to another. These errors can

be stabilized by the previously designed controller without changing form since the proposed controller will stabilize the formation errors globally. Figure 10 depicts a transformation between rigid formations. Six agents were first driven into a hexagonal rigid formation followed by a straight line formation into a triangular shape. During the first 10 seconds the six agents form a hexagonal formation starting from the initial conditions in Table III, then this hexagonal formation is maintained for another 10 seconds. In order to escape obstacles which are shown as gray squares in Fig.10, agents form a line formation for the next 30 seconds. Last, agents form triangular formation. Each formation specifications are shown in Table III. Figure 11 shows formation errors of the first and the second agents. The others are omitted because they are quite similar. Formation errors occur at the initial time, at 20 secs., and 50 secs. due to formation shape change.

Table III. Initial Conditions

States	$i=1$	$i=2$	$i=3$	$i=4$	$i=5$	$i=6$	$i=v1$	$i=v2$
$x_i(m)$	11	10	-13	12	4	32	-10	0
$y_i(m)$	-32	-48	-56	-56	-37	-48	-20	-20
$\theta_i(rad)$	0.2	$-\pi$	1.2	-0.7	$-\frac{\pi}{2}$	2.2	$\frac{\pi}{2}$	$\frac{\pi}{2}$
$v_i(m/sec)$	1	2	3	4	5	6	1	2

E. Summary

In this chapter we considered several issues which appear when the control scheme proposed in chapter II is applied to practical situations. The first issue is singularity in computation. Since the values of control input are determined by matrix inversion, computation is impossible when the matrix is singular. A discontinuous controller was proposed to avoid matrix inversion. This alternative controller stabilizes formation

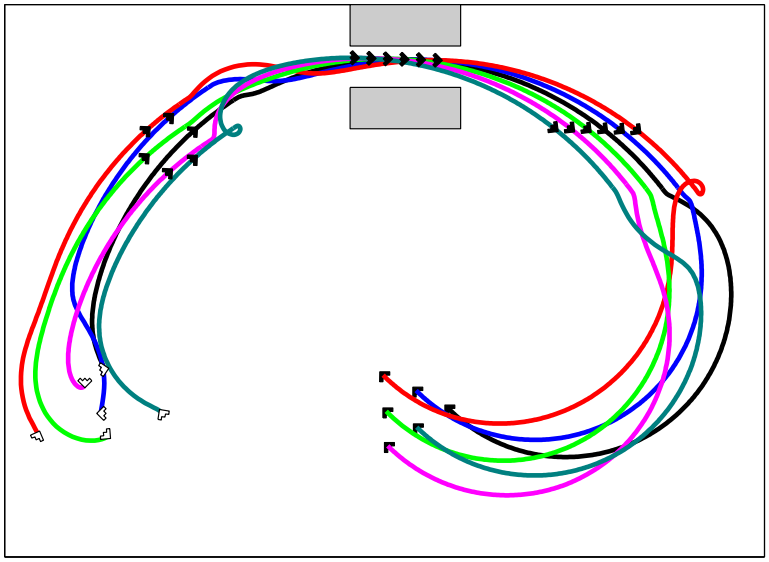

Fig. 10. Transformation

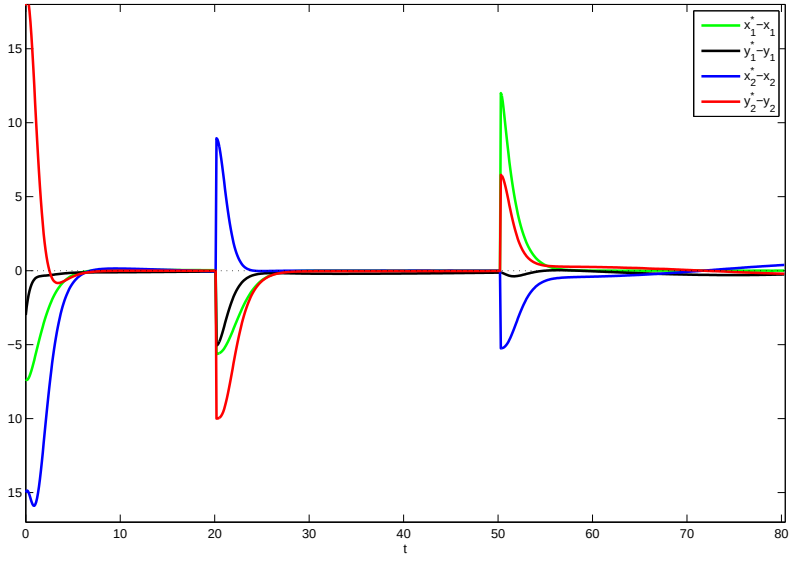

Fig. 11. Formation errors during transformation

Table IV. Specification of Formation

Hexagonal formation						
	$i=1$	$i=2$	$i=3$	$i=4$	$i=5$	$i=6$
$d_i(m)$	10	10	10	10	10	10
$\alpha_i(rad)$	$\frac{\pi}{6}$	$\frac{\pi}{2}$	$\frac{5\pi}{6}$	$-\frac{5\pi}{6}$	$-\frac{\pi}{2}$	$-\frac{\pi}{6}$
Line formation						
	$i=1$	$i=2$	$i=3$	$i=4$	$i=5$	$i=6$
$d_i(m)$	3	9	15	3	9	15
$\alpha_i(rad)$	0	0	0	π	π	π
Triangular formation						
	$i=1$	$i=2$	$i=3$	$i=4$	$i=5$	$i=6$
$d_i(m)$	15	$15\sin(\frac{\pi}{6})$	15	$15\sin(\frac{\pi}{6})$	15	$15\sin(\frac{\pi}{6})$
$\alpha_i(rad)$	0	$\frac{\pi}{3}$	$\frac{2\pi}{3}$	π	$-\frac{2\pi}{3}$	$-\frac{\pi}{3}$

errors asymptotically when a formation is stationary. The second issue is robust stability with uncertain terms in agent dynamics. By Lyapunov redesign method, the controller is modified to stabilize a formation when uncertain terms exist in the dynamics of agents. The third, we consider guiding techniques for a rigid formation. Utilizing two virtual leaders, we can drive a rigid formation with desired linear velocity and angular velocity. Last, transformation between rigid formations is considered. The proposed scheme in chapter II can be directly applied to this application without change, and it was shown that the designed controllers succeed in stabilizing formation error caused by formation change.

CHAPTER IV

SURVEILLANCE

The scenario under consideration in this chapter is one of Cooperative Moving Target Engagement (**CMTE**). Here several small Unmanned Air Vehicles (**UAV**s) with small-area Ground Moving Target Indication (**GMTI**) radars and **GPS** guided ground-attack weapons are tasked to cooperatively track and attack ground moving targets. In addition, a stand-off **UAV** with a wide-area **GMTI** radar cooperates with the small **UAV**s to detect ground moving targets. In practical situations there could be instances when the moving target is outside the view of small-area **GMTI** radars when a finite number of **UAV**s are used. The main motivation here is to develop algorithms that determine the minimum number of **UAV**s needed to monitor the moving target and to plan the path of the **UAV**s in an efficient way. There are several issues associated with this problem. The first issue is how to assign a group of **UAV**s and how to quantify the efficiency of assigning algorithms. The second is how to design the path of the **UAV**s in order to decrease redundancy. The third is how to formulate this problem considering constraints caused by dynamics of **UAV**s and the limitation of **GMTI** radar. Here our focus is on the development of an algorithm which determines the minimal number of **UAV**s for this mission. That algorithm should be computationally attractive and applicable to in real-time situations. In order to mitigate the limitation of **GMTI** radar, it is assumed that **GMTI** radar can detect moving target regardless of its direction. Also, the speed range of moving target is assumed to be known a-priori.

A. Problem Statement

Now we consider the following scenario based on the formation control scheme proposed in chapter **II**. Consider a task where multiple **UAV**s are assigned to track a ground moving target. Each **UAV** has a specific sensor footprint provided by a sensor fixed on it. The sensor footprint is limited in range and in angle. The direction of the sensor footprint is confined by the pose of the **UAV**. Also, each **UAV** can not move backward. Namely, the speed of the i^{th} **UAV**, v_i is assumed always positive. That is the main reason why a single **UAV** cannot track a moving target for all time on its own. If one agent fails to track a moving target, multiple agents should be assigned to fulfil the task.

B. Approach

The goal is to develop a scheme that determines the minimal number of agents required for this task. Let us assume that all **UAV**'s and a ground moving target are confined in $\mathcal{R}^2$. This assumption means that the area of the sensor footprint will not change due to the motion of the agent. Let $\mathbf{r}_t$ be the position vector of the ground moving target T, and $\mathbf{r}_i$ be the position vector of the i^{th} **UAV**. L_{min} and L_{max} denote the minimum sensor range and the maximum sensor range respectively. Let us assume that N **UAV**s form a rigid formation, and the shape of the rigid formation is a circle. The center of the circle O_B is denoted by the position vector $\mathbf{r}_{O_B}$ with respect to the inertial frame, and its radius is d. O_B is assumed to coincide with the position of the ground moving target T and is given by

$$[\mathbf{r}_{O_B}]_I = [\mathbf{r}_t]_I \quad . \tag{4.1}$$

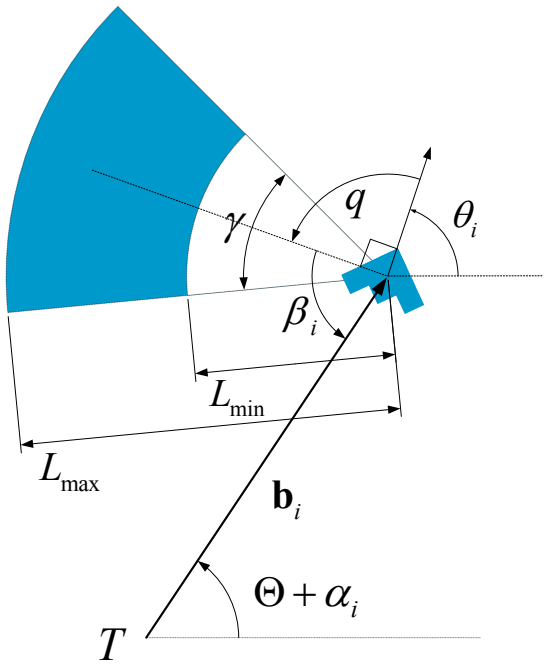

Fig. 12. Characterization of β_i: Gray sector stands for the footprint of the sensor.

If the value of d is chosen to lie between L_{min} and L_{max}, as in Fig.12, then N **UAV**s will lie on the circle whose radius is d and whose center coincides with the target. Next we consider the distribution of the N **UAV**s on this circle so that the target falls within at least one of the sensor footprints of the cooperating **UAV**s. Suppose the target as well as the i^{th} **UAV** has nonholonomic kinematics of a unicycle given by;

$$\begin{bmatrix} \dot{x}_t \\ \dot{y}_t \\ \dot{\theta}_t \end{bmatrix} = \begin{bmatrix} v_t \cos\theta_t \\ v_t \sin\theta_t \\ \omega_t \end{bmatrix}, \qquad \begin{bmatrix} \dot{x}_i \\ \dot{y}_i \\ \dot{\theta}_i \end{bmatrix} = \begin{bmatrix} v_i \cos\theta_i \\ v_i \sin\theta_i \\ \omega_i \end{bmatrix} \qquad \begin{matrix} i = 1, 2, \cdots, N \\ V_{min} \le v_i \le V_{max} \end{matrix} \tag{4.2}$$

where $v_i \geq 0$. If all **UAV**s construct the circular rigid formation by the controller developed in the previous chapter(Ch.III), all formation errors will be small enough

and may be neglected.

$$\mathbf{E}_i = 0, \qquad i = 1, 2, \cdots, N \tag{4.3}$$

Also, all **UAV**s move as points in a single **VS**. A local frame B is assumed fixed to the **VS** with its origin located at the virtual point O_B. Let let $[\mathbf{R}]$ be the coordinate transformation matrix from frame B to the inertial frame I. Let $[\mathbf{r}_t]_I = [x_t, y_t]^T$ and $[\mathbf{r}_i]_I = [x_i, y_i]^T$. Then, $[\mathbf{r}_i]_I = [\mathbf{r}_t]_I + [\mathbf{R}][\mathbf{b}_i]_B$ which yields;

$$\begin{aligned} \dot{x}_i &= \dot{x}_t - \dot{\Theta} d \sin(\Theta + \alpha_i) \\ \dot{y}_i &= \dot{y}_t + \dot{\Theta} d \cos(\Theta + \alpha_i) \end{aligned} \tag{4.4}$$

where $\alpha_i = \angle([\mathbf{r}_i]_B)$. Combining Eq.(4.2) and Eq.(4.4), the relationship between the velocity of the i^{th} **UAV** and the velocity of ground moving target are represented by;

$$\begin{aligned} v_i \cos\theta_i &= v_t \cos\theta_t - \dot{\Theta} d \sin(\Theta + \alpha_i) \\ v_i \sin\theta_i &= v_t \sin\theta_t + \dot{\Theta} d \cos(\Theta + \alpha_i) \end{aligned} \tag{4.5}$$

1. Separation Angle

Even if all **UAV**s maintain a constant distance d between target and itself, there is one more condition needed for the moving target to fall inside one of the sensor footprints of **UAV**s. Since sensors of each **UAV**s are limited in angle also, the moving target should be located between angle limitation in order that one of the **UAV**s can detect the moving target. The separation angle β_i in Fig.12 shows how much the center of the sensor footprint deviates off the target. If $|\beta_i| \leq \frac{\gamma}{2}$, the moving target falls in the sensor footprint of the i^{th} **UAV**. In this research, q is considered a constant value of $\frac{\pi}{2}$ for simplicity. Let us define the separation angle β_i as follows:

$$\beta_i = q - \theta_i + \Theta + \alpha_i \tag{4.6}$$

The separation angle is a function of θ_i and Θ. α_i is a constant when the distributed pattern of N **UAV**s is fixed. q is also a constant because the sensor is fixed on the **UAV** body. Since each **UAV** maintains the distance d between a moving target and itself, the separation angle can be expressed by the linear velocity and orientation of the moving target. Using Eq.(4.5) $\tan(\beta_i)$ can be represented by

$$\begin{aligned}
\cos\beta_i &= \cos(\frac{\pi}{2} - \theta_i + \Theta + \alpha_i) \\
&= \sin\theta_i \cos(\Theta + alpha_i) - \cos\theta_i \sin(\Theta + alpha_i) \\
&= \frac{1}{v_i}(\dot{\Theta}d - v_t \sin(\Theta + \alpha_i - \theta_t)), \\
\sin\beta_i &= \sin(\frac{\pi}{2} - \theta_i + \Theta + \alpha_i) \\
&= \cos\theta_i \cos(\Theta + alpha_i) + \cos\theta_i \cos(\Theta + alpha_i) \\
&= \frac{1}{v_i} v_t \cos(\Theta + \alpha_i - \theta_t), \\
\tan\beta_i &= \frac{v_t \cos(\Theta + \alpha_i - \theta_t)}{\dot{\Theta}d - v_t \sin(\Theta + \alpha_i - \theta_t)}.
\end{aligned} \tag{4.7}$$

By denoting $\Theta + \alpha_i - \theta_t$ as κ_i β_i can be written as

$$\tan\beta_i = \frac{\sin\beta_i}{\cos\beta_i} = \frac{v_t \cos\kappa_i}{\dot{\Theta}d - v_t \sin\kappa_i} \quad . \tag{4.8}$$

2. Feasible v_t

In practical situations, there are limitations in control inputs. Suppose that the linear velocity of the i^{th} agent v_i is bounded by the upper limit V_{max} and the lower limit V_{min}, then feasible values of v_t should be considered. If $|v_t|$ is greater than V_{max}, it is impossible that any agent maintains a constant distance between target and itself. Now let us consider feasible values of v_t taking into consideration the constraints

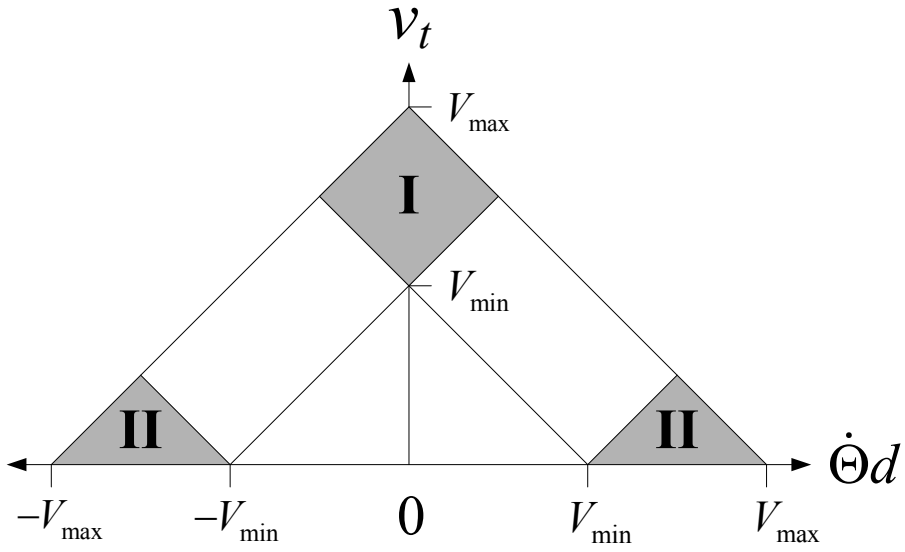

Fig. 13. Feasible region of v_t and $\dot{\Theta}$

between agents and target. Equation(4.4) and Eq.(4.2) yield the following;

$$v_i^2 = v_t^2 + \dot{\Theta}^2 d_i^2 + 2 v_i \dot{\Theta} d \sin(\theta_t + \Theta + \alpha_i)) \qquad . \tag{4.9}$$

One can find the feasible region for v_t and $\dot{\Theta}$ from Eq. (4.9) leading to the following;

$$\begin{aligned} (v_t - |\dot{\Theta}|d)^2 &\geq V_{min}^2 \\ (v_t + |\dot{\Theta}|d)^2 &\leq V_{max}^2 \end{aligned} \tag{4.10}$$

This region is shown graphically in Fig.13. Since regions **I** and **II** in Fig.13 are disconnected, the controller will be discontinuous if the values of $|v_t|$ varies from region **I** to region **II** or vice versa. So, the value of v_t is assumed to remain in region **I** or **II** exclusively. Let us call case-**I** situation where the pair $(v_t, \dot{\Theta}d)$ remains exclusively in region **I** and case-**II** when it remains exclusively in region **II**. Let us consider surveillance problem in case-**I** first, then consider it in case-**II**.

3. Case-**I**

In case-**I**, v_t is assumed to have a value between V_{max} and V_{min}, and $\dot{\Theta}d$ is between $-\frac{V_{max}-V_{min}}{2}$ and $\frac{V_{max}-V_{min}}{2}$. Let us consider the situation where N **UAV**s are distributed uniformly on a circle whose radius is d and whose center coincides with the target. This can be expressed by the number of **UAV**s N and distribution pattern $\alpha_{i+1} = \alpha_i + \Delta\alpha (i = 1, 2, ..., N-1)$ where $\Delta\alpha$ denotes the angular displacement. If $\dot{\Theta} = 0$, then $\frac{\partial\beta_i}{\partial\kappa_i} = 1$ by Eq.(4.8) and N can be determined by $\lceil\frac{2\pi}{\gamma}\rceil$ where a ceiling function $\lceil\cdot\rceil$ is defined by the following;

Definition 6 (Ceiling Function $\lceil\cdot\rceil$) $\lceil x\rceil = \min\{n \in \mathcal{Z} | x \leq n, x \in \mathcal{R}\}$.

This is explained in Fig.14(a). Sensor footprints are connected to each other and there is no gap between them, and one separation angle has a value between $-\frac{\gamma}{2}$ and $\frac{\gamma}{2}$. Therefore $N(= \lceil\frac{2\pi}{\gamma}\rceil)$ agents can monitor the moving target for all time. However, $\lceil\frac{2pi}{\gamma}\rceil$ is not enough for N when $\dot{\Theta} \neq 0$. The reason being that the partial derivative of β_i with respect to κ_i is not always 1 when $\dot{\Theta} \neq 0$. Figure 14(b) shows that there is some gap between sensor footprints when $\frac{\partial\beta_i}{\partial\kappa_i} \neq 1$, and there is an instance when none of $|\beta_i|$s is smaller than $\frac{\gamma}{2}$. Consequently, all the agents fail to detect the moving target at a certain instance.

That is the reason why we need to increase the number of **UAV**s, considering the maximum value of $|\frac{\partial\beta_i}{\partial\kappa_i}|$.

$$\frac{\partial\beta_i}{\partial\kappa_i} = \frac{v_t^2 - v_t\dot{\Theta}dsin\kappa_i}{\dot{\Theta}^2d^2 + v_t^2 - 2v_t\dot{\Theta}d\sin\kappa_i} \tag{4.11}$$

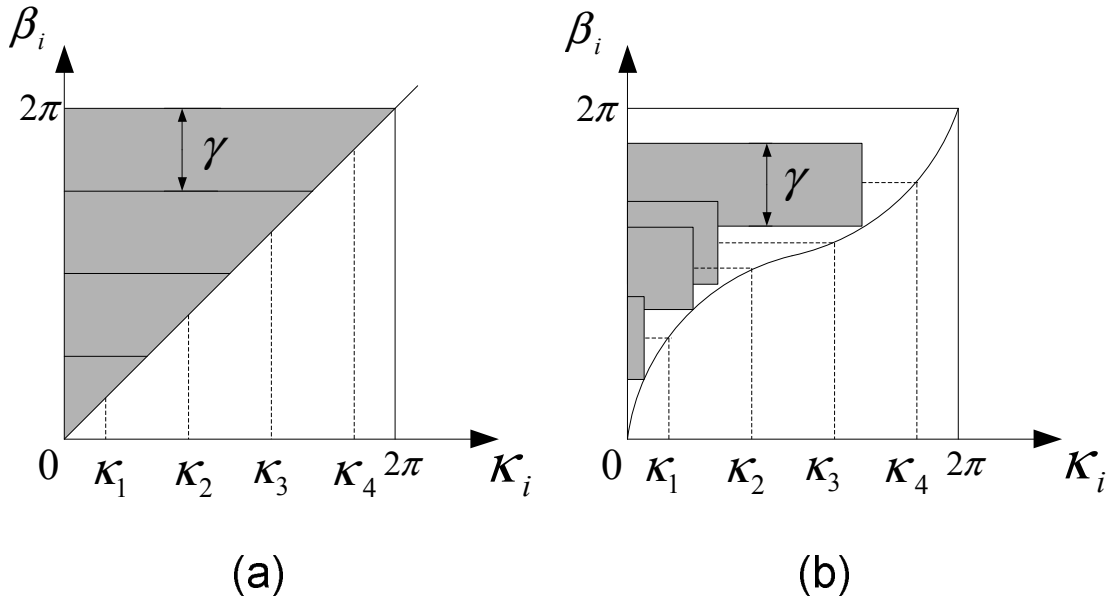

Fig. 14. The relationship between β_i and κ_i when $\frac{\partial \beta_i}{\partial \kappa_i} = 1$ (a) and $\frac{\partial \beta_i}{\partial \kappa_i} \neq 1$ (b)

and $\frac{\partial \beta_i}{\partial \kappa_i}$ always has a positive value in case-**I**, since $v_t \geq |\dot{\Theta}|d$.

$$\begin{aligned} \max_{\text{case}-\mathbf{I}} \left(\left| \frac{\partial \beta_i}{\partial \kappa_i} \right| \right) &= \max_{\text{case}-\mathbf{I}} \left(\frac{v_t^2 - v_t \dot{\Theta} d \sin \kappa_i}{\dot{\Theta}^2 d_i^2 + v_t^2 - 2 v_t \dot{\Theta} d \sin \kappa_i} \right) \\ &= \max_{\text{case}-\mathbf{I}} \left(\frac{v_t}{v_t - |\dot{\Theta}| d} \right) \\ &= \frac{V_{max} + V_{min}}{2 V_{min}} > 1 \end{aligned} \tag{4.12}$$

$\left| \frac{\partial \beta_i}{\partial \kappa_i} \right|$ has the maximum value in case-**I** where $v_t = \frac{V_{max}+V_{min}}{2}$ and $|\dot{\Theta}|d = \frac{V_{max}-V_{min}}{2}$. Now the minimal number of the **UAV**s in case-**I**, N_I^* and angle displacement $\Delta\alpha$ can be represented by the following;

$$\begin{aligned} N_I^* &= \left\lceil \frac{2\pi \max_{\text{case}-\mathbf{I}} \left(\left| \frac{\partial \beta_i}{\partial \kappa_i} \right| \right)}{\gamma} \right\rceil = \left\lceil \frac{\pi (V_{max} + V_{min})}{\gamma V_{min}} \right\rceil \\ \Delta\alpha &= \frac{2\pi}{N_I^*} \end{aligned} \tag{4.13}$$

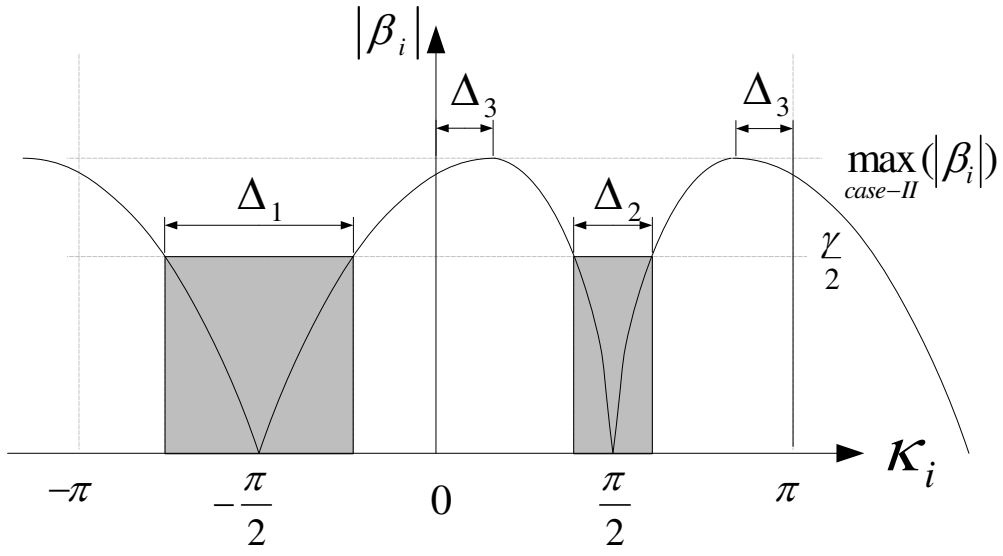

Fig. 15. $|\beta_i|$ in case-**II**

4. Case-**II**

Now we consider the minimal number of **UAV**s in case-**II**. In this case, the ground moving target speed is much smaller than speeds of **UAV**s, while the speed of moving target is similar to that of **UAV**s in case-**I**. From (4.11) the value of $|\beta_i|$ is limited in case-**II**, and it has the maximum value when $\sin\kappa_i = \frac{v_t}{\dot{\Theta}d}$. The maximum value of $|\beta_i|$ in case-**II** is the following;

$$\begin{aligned} \max_{\text{case}-\mathbf{II}}(|\beta_i|) &= \arctan\left(\max_{\text{case-II}}\left(\frac{v_t}{\sqrt{(\dot{\Theta}d)^2-(v_t)^2}}\right)\right) \\ &= \arctan\left(\frac{V_{max}-V_{min}}{2\sqrt{V_{max}V_{min}}}\right) \end{aligned} \tag{4.14}$$

β_i can vary only between $-\arctan\left(\frac{V_{max}-V_{min}}{2\sqrt{V_{max}V_{min}}}\right)$ and $\arctan\left(\frac{V_{max}-V_{min}}{2\sqrt{V_{max}V_{min}}}\right)$ in case-**II**. $|\beta_i|$ in case-**II** can be represented by Fig.15 graphically. If one half of the sensor coverage angle $\frac{\gamma}{2}$ is greater than $\max(|\beta_i|)$, then only one **UAV** is required to track

the moving target. However, if κ_i lies in $[-\frac{\pi}{2}-\frac{\Delta_1}{2}, -\frac{\pi}{2}+\frac{\Delta_1}{2}]$ or $[\frac{\pi}{2}-\frac{\Delta_2}{2}, \frac{\pi}{2}+\frac{\Delta_2}{2}]$, then the i^{th} **UAV** can detect the moving target when $\frac{\gamma}{2} < \max_{\text{case}-\mathbf{II}} |\beta_i|$. Since $\Delta_3 = \sin^{-1}(\frac{v_t}{\dot{\Theta}d})$ is always greater than zero in case-II, Δ_1 is always greater than Δ_2. Also an $|\beta_i|$ is symmetric with respect to $\kappa_i = \frac{\pi}{2} + n\pi$ where n is integer. Let us call N^*_{II} as the minimal number of **UAV** in in case-II. If N^*_{II} **UAV**s are distributed equally spaced on the half circle, and the angular displacement $\Delta\alpha$ is smaller than Δ_2, and at least one **UAV** can detect the moving target, then we can propose the following scheme for case-II.

$$
\begin{aligned}
N^*_{II} &= \begin{cases} \left\lceil \dfrac{\pi}{\min(\Delta_2)} \right\rceil & \text{if } \dfrac{\gamma}{2} < \max\limits_{\text{case}-\mathbf{II}} (|\beta_i|) \\ 1 & \text{if } \dfrac{\gamma}{2} \geq \max\limits_{\text{case}-\mathbf{II}} (|\beta_i|) \end{cases} \\
\Delta\alpha &= \frac{\pi}{N^*_{II}}
\end{aligned}
\tag{4.15}
$$

where

$$
\Delta_2 = 2\arcsin(\frac{\dot{\Theta}d}{v_t}\sin\frac{\gamma}{2}) - \gamma \quad .
$$

The minimum value of Δ_2 is determined when $\dot{\Theta}d = \frac{V_{max}+V_{min}}{2}$ and $v_t = \frac{V_{max}-V_{min}}{2}$. Therefore, the scheme proposed in Eq.4.15 can be expressed in the following form.

$$
\begin{aligned}
N^*_{II} &= \begin{cases} \left\lceil \dfrac{\pi}{2\arcsin(\frac{V_{max}+V_{min}}{V_{max}-V_{min}}\sin\frac{\gamma}{2}) - \gamma} \right\rceil & \text{if } \dfrac{\gamma}{2} < \max\limits_{\text{case}-\mathbf{II}} (|\beta_i|) \\ 1 & \text{if } \dfrac{\gamma}{2} \geq \max\limits_{\text{case}-\mathbf{II}} (|\beta_i|) \end{cases} \\
\Delta\alpha &= \frac{\pi}{N^*_{II}}
\end{aligned}
\tag{4.16}
$$

C. Summary

We developed an algorithm which determines a minimal number of **UAV**s for surveillance of a moving target in this chapter. The proposed algorithm determines the minimal number depending on the speed range of moving target. The feasible speed

of moving target was considered, and the feasible pair $(v_t, \dot{\Theta}d)$ is not continuous as shown in Fig.13. The minimal number of **UAV**s N^* and the distributed pattern $\Delta\alpha$ can be rewritten in the following form.

$$N^* = \begin{cases} \left\lceil \frac{\pi}{2\arcsin(\frac{V_{max}+V_{min}}{V_{max}-V_{min}}\sin\frac{\gamma}{2})-\gamma} \right\rceil & \text{if } v_t \le \frac{V_{max}-V_{min}}{2} \text{ and } \frac{\gamma}{2} < \tan^{-1}(\frac{V_{max}-V_{min}}{2\sqrt{V_{max}V_{min}}}) \\ 1 & \text{if } v_t \le \frac{V_{max}-V_{min}}{2} \text{ and } \frac{\gamma}{2} \ge \tan^{-1}(\frac{V_{max}-V_{min}}{2\sqrt{V_{max}V_{min}}}) \\ \frac{\pi(V_{max}+V_{min})}{\gamma V_{min}} & \text{if } v_t \ge V_{min} \\ undefined & \text{if } V_{min} \ge v_t \ge \frac{V_{max}-V_{min}}{2} \end{cases} \tag{4.17}$$

$$\Delta\alpha = \begin{cases} \frac{\pi}{N^*} & \text{if } v_t \le \frac{V_{max}-V_{min}}{2} \\ \frac{2\pi}{N^*} & \text{if } v_t \ge V_{min} \end{cases}$$

A remarkable fact in the proposed algorithm is that the computation takes $O(1)$ time, whereas algorithms based on optimization techniques take $O(N^N)$ time for N agents. The proposed algorithm requires the speed range of the moving target, and it is independent of the number of agents N. However, the proposed algorithm can not decide the minimal number of **UAV**s when $V_{min} \ge v_t \ge \frac{V_{max}-V_{min}}{2}$. The reason is that **UAV**s can not maintain a constant distance d when $V_{min} \ge v_t \ge \frac{V_{max}-V_{min}}{2}$. The validity of this algorithm was verified in the following simulations.

D. Simulation Results

Figure 16(a) shows that all of the **UAV**s fail to detect the moving target when $\gamma = \frac{\pi}{2}$, $N = 4$ and $\alpha_{i+1} = \alpha_i + \frac{\pi}{2}(i = 1, 2, 3)$. The moving target is shown in Fig.16 as $*$, and the blue sectors stand for the footprints of the sensors. Figure 16 (b) shows that N_I^* **UAV**s can detect the moving target successfully. In this simulation, control bounds V_{max}, and V_{min} were chosen to be 13m/sec, and 7m/sec respectively. The

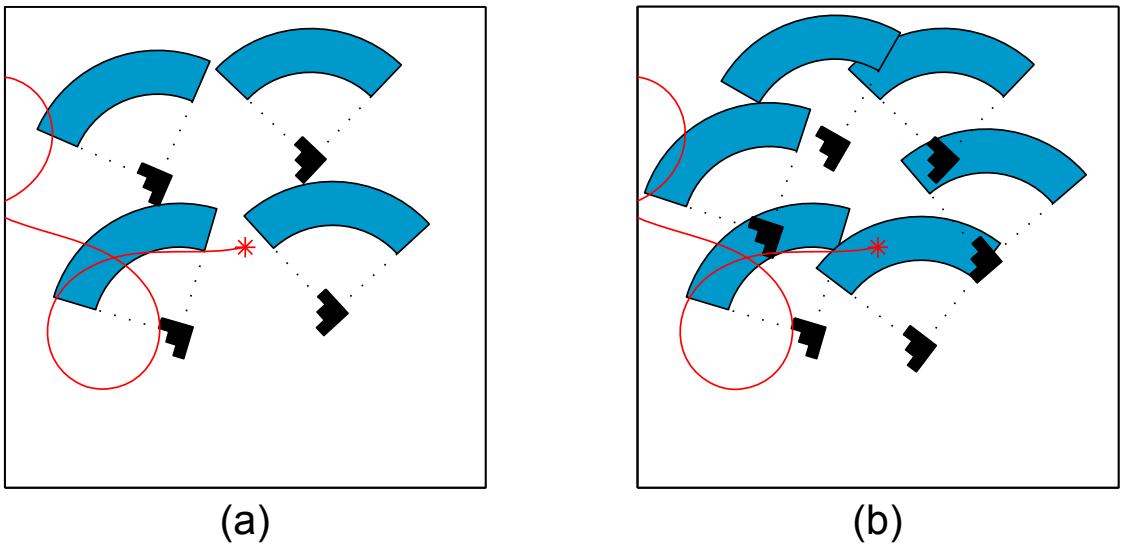

Fig. 16. $*$ represents a moving target. (a) shows that $N(=\lceil\frac{2\pi}{\gamma}\rceil)$ **UAV**'s fail to detect the moving target. (b) shows that N_I^* **UAV**'s succeed in detecting the moving target.

sensor footprint was chosen as $\gamma = \frac{\pi}{2}$rad, L_{min}=8m, and L_{max}=12m. The number N_I^* was determined to be 6 by Eq.(4.13). Six **UAV**s form a circular formation whose radius is d=10m and whose center coincides with the target. The ground moving target was assumed to move with the linear velocity $v_t = 10m/sec$ and the angular velocity $w_t = 2\sin(\frac{2}{3}t)$. The angular velocity of the formation $\dot{\Theta}$ was chosen to be -0.3rad/sec. As we saw in Fig. 13, the value of $|\dot{\Theta}|$ should not be greater than $\frac{V_{max}-V_{min}}{2d}$=0.3rad/sec. Figure 17 shows N_{II}^* **UAV**s successfully detecting the moving target when $\frac{\gamma}{2} < \max_{\text{case}-\mathbf{II}}(|\beta_i|)$. In this simulation, γ was chosen to be 0.4rad. Control bounds V_{max}, and V_{min} were chosen to be 13m/sec, and 7m/sec respectively. The range of sensor footprint was chosen by $\gamma = \frac{\pi}{2}$rad, L_{min}=8m, and L_{max}=12m. The number N_{II}^* was determined to be 3 by Eq.(4.16). Three **UAV**s fall in a circular formation whose radius is d=10m and whose center coincides with the target. The angular displacement $\Delta\alpha$ is determined as $\frac{\pi}{3}$ from Eq.(4.16) and α_i was chosen to

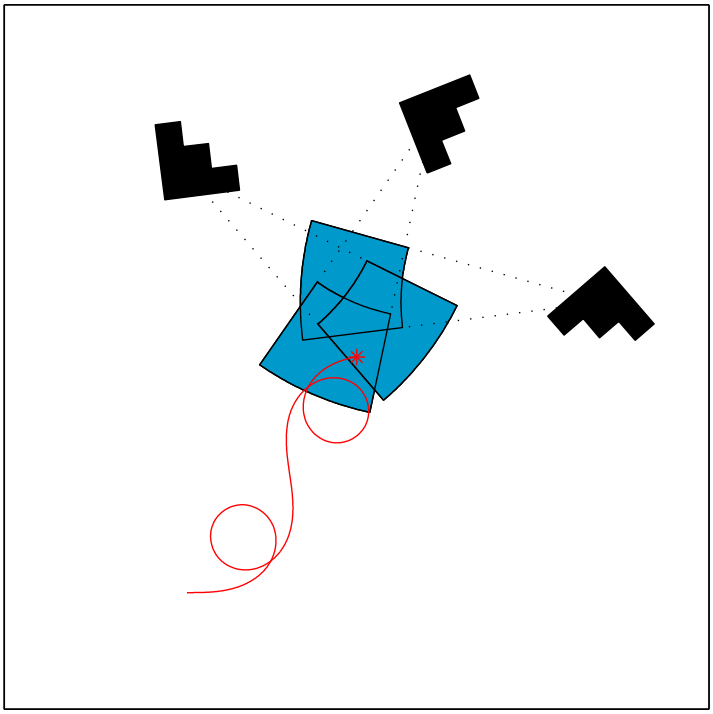

Fig. 17. N_{II}^{*} **UAV**'s succeed in detecting the moving target.

be $\frac{\pi}{4}$. The ground moving target was assumed to move with the linear velocity $v_t = 2.5m/sec$ and the angular velocity $w_t = 2\sin(\frac{t}{2})$. The angular velocity of the formation $\dot{\Theta}$ was chosen to be 1rad/sec. Additionally, $\dot{\Theta}$ must be positive in case-**II**. The reason being that q, as shown in Fig.12, is a constant equal to $\frac{\pi}{2}$. If $\dot{\Theta}$ has a negative value, $\beta_i \notin (-\frac{\pi}{2}, \frac{\pi}{2})$ in case-**II** which can easily be determined using (4.8), and none of the **UAV**s can detect the moving target.

CHAPTER V

CONCLUSION

A salable scheme was proposed for rigid formation construction by a novel representation of formation constraints. This representation is independent of the number of agents in a formation and the resulting control algorithm is scalable. The proposed approach is based on a fusion of leader-follower and virtual reference approach. The group behavior is directed by specifying the behavior of virtual agents in the proposed method. Also desired positions of all the agents in a rigid formation can be expressed by the position of virtual agents since the virtual structure constructed by virtual agents behaves like a rigid body. However, inter-collision avoidance was not considered in the proposed scheme. Collision avoidance may be handled by the potential field approach or the homotopy approach based on homotopy of polynomials in [33]. A challenging issue is how to utilize these approaches in the proposed scheme without loss of scalability. The potential field approach and homotopy approach require all the position of agents in order that a trajectory of one agent is determined. This conflicts with the condition of formation constraints for scalability algorithm. Future research should include a scalable algorithm considering inter-collision avoidance. This work will be valuable when the algorithm is applied to a large number of agent systems.

Formation errors are exponentially and globally stabilized by the proposed control laws. A nonholonomic model was considered for agents, and the proposed controller was built by feedback linearization. Exponential stability of formation errors was shown by Lyapunov stability theory and verified by simulations. When the angular velocity of the formation $\dot{\Theta}$ and the linear velocity of the formation v_{VS} are very small, ill condition appears in matrix inversion. An alternative controller for this situation was developed by nonlinear coordinate transformation and the formation errors

are stabilized by the alternate discontinuous controller when $\dot{\Theta}^2 + v_{VS}^2$ is very small. Robust stability is approached with Lyapunov redesign method. We assumed that the uncertainties δ_i satisfy the inequality $\|\delta_i\| \leq \rho_i + k_i\|\Delta\mathbf{u}_i\|$. Under the assumption, the proposed controller can stabilize a formation with uncertainties in the dynamics of agents. From an implementation point of view, the drawback of the proposed controller is that the feasibility of the control inputs was not considered. Although the positions of virtual agents were chosen to easily detect whether control inputs of actual agents exceed control bounds or not, it was useful to prove local stability of a formation with control bounds. Future work should consider global stability of a formation with nonholonomic constraints and control bounds.

The surveillance problem, especially ground moving target engagement problem was considered as an application of the formation control scheme proposed in this research. The minimal number of agents required for surveillance of a moving target, was determined by the proposed scheme. It was assumed that the speed range of the moving target is known a-priori. Detectable speed ranges of moving targets were separated into two regions. The proposed algorithm determines the minimal number of agents according to these regions.Although the number of agents returned by the proposed scheme is not optimal, it still is an attractive scheme because computation time $T(N)$ is $O(1)$. The reason being that the computations require only the controller bounds for each of the agents and is independent of the number of agents N, while algorithms based on optimization techniques have order N^N times complexity for N agents. The weakness of the proposed algorithm is that it cannot determine the minimal number of agents when the target speed is between V_{min} and $\frac{V_{max}-V_{min}}{2}$. The reason is that all the agents cannot maintain a constant distance between target and itself in that situation. Future work should consider algorithms which determine minimal number of agents needed for monitoring a moving target when $V_{min} \geq v_t \geq$

$\frac{V_{max}-V_{min}}{2}$. Another interesting future work is the consideration of heterogeneous systems for agents and targets. This is important in applications where agents are dissimilar to each other in dynamics or in sensor assets and the number of targets is greater than one. Since the proposed scheme is applicable to only one moving target, a modified algorithm is required such that moving targets are assigned to a proper group of agents by the algorithm.

REFERENCES

[1] D. Fox, W. Burgard, H. Kruppa, and S. Thrun, "Collaborative multi-robot exploration," *Autonomous Robots*, vol. 8, no. 3, pp. 325–344, 2000.

[2] H. Kitano, S. Tadokoro, I. Noda, H. Matsubara, T. Takahashi, A. Shinjou, and S. Shimada, "Robocup rescue: search and rescue in large-scale disasters as adomain for autonomous agents research," in *Proceedings of the IEEE International Conference on Systems, Man, and Cybernetics*, 1999, vol. 6, pp. 739–743.

[3] R.T. Collins, A.J. Lipton, H. Fujiyoshi, and T. Kanade, "Algorithms for cooperative multisensor surveillance," in *Proceedings of the IEEE*, 2001, vol. 89, pp. 1456–1477.

[4] D.B. Kingston and C.J. Schumacher, "Time-dependent cooperative assignment," in *Proceedings of the American Control Conference*, 2005, pp. 4084–4089.

[5] O. Shehory and S. Kraus, "Methods for task allocation via agent coalition formation," *Artificial Intelligence*, vol. 101, no. 1-2, pp. 165–200, 1998.

[6] J.A. Fax and R.M. Murray, "Information flow and cooperative control of vehicle formations," *IEEE Transactions on Automatic Control*, vol. 49, no. 9, pp. 1465–1476, 2004.

[7] M.J. Mataric, M. Nilsson, and K. Simsarian, "Cooperative multi-robot box-pushing," in *Proceedings of the IEEE/RSJ International Conference on Intelligent Robots and Systems*, 1995, pp. 556–561.

[8] C.R. Kube and E. Bonabeau, "Cooperative transport by ants and robots," *Robotics and Autonomous Systems*, vol. 30, pp. 85–101, 2000.

[9] W. Ren and R.W. Beard, "Decentralized scheme for spacecraft formation flying via the virtual structure approach," *Journal of Guidance, Control, and Dynamics*, vol. 27, no. 1, pp. 73–82, 2004.

[10] F. Giulietti, L. Pollini, and M. Innocenti, "Autonomous formation flight," *IEEE Control Systems Magazine*, vol. 20, no. 6, pp. 34–44, 2000.

[11] D. Parsons and J. Canny, "A motion planner for multiple mobile robots," in *Proceedings of the IEEE International Conference on Robotics and Automation*, 1990, pp. 8–13.

[12] E.F. Gurewitz and G.Y. Wong, "Parallel algorithms for one and two-vehicle navigation," in *Proceedings of the Fifth Distributed Memory Computing Conference*, 1990, pp. 140–147.

[13] A.K. Das, R. Fierro, V. Kumar, J.P. Ostrowski, J. Spletzer, and C.J. Taylor, "A vision-based formation control framework," *IEEE Transactions on Robotics and Automation*, vol. 18, no. 5, pp. 813–825, 2002.

[14] J.P. Desai, J.P. Ostrowski, and V. Kumar, "Modeling and control of formations of nonholonomic mobile robots," *IEEE Transactions on Robotics and Automation*, vol. 17, no. 6, pp. 905–908, 2001.

[15] P.K.C. Wang, "Navigation strategies for multiple autonomous mobile robots moving in formation," in *Proceedings of the IEEE/RSJ International Workshop on Intelligent Robots and Systems*, 1989, pp. 486–493.

[16] H. Yamaguchi, T. Arai, and G. Beni, "A distributed control scheme for multiple robotic vehicles to make group formations," *Robotics and Autonomous Systems*, vol. 36, no. 4, pp. 125–147, 2001.

[17] T. Balch and R.C. Arkin, "Behavior-based formation control for multirobot teams," *IEEE Transactions on Robotics and Automation*, vol. 14, no. 6, pp. 926–939, 1998.

[18] M.A. Lewis and K.H. Tan, "High precision formation control of mobile robots using virtual structures," *Autonomous Robots*, vol. 4, no. 4, pp. 387–403, 1997.

[19] J. Lin, A.S. Morse, and B.D.O. Anderson, "The multi-agent rendezvous problem," in *Proceedings. 42nd IEEE Conference on Decision and Control*, 2003, vol. 2, pp. 1508–1513.

[20] A. Jadbabaie, J. Lin, and A. S. Morse, "Coordination of groups of mobile autonomous agents using nearest neighbor rules," *IEEE Transactions on Automatic Control*, vol. 48, no. 6, pp. 988–1001, 2003.

[21] D.H.A. Maithripala, "Coordinated multi-agent motion planning for formation control," Ph.D. Dissertation, Texas A&M University, College Station, Texas, 2008.

[22] D.H.A. Maithripala, D.H.S. Maithripala, and S. Jayasuriya, "Unifying geometric approach to real-time formation control," in *Proceedings of the American Control Conference*, 2008, pp. 789–794.

[23] D.H.A. Maithripala and S. Jayasuriya, "Rigid formation keeping and formation reconfiguration of multi-agent systems," *IFAC World Congr*, pp. 5155–5160, 2008.

[24] M. Egerstedt and X. Hu, "Formation constrained multi-agent control," *IEEE Transactions on Robotics and Automation*, vol. 17, no. 6, pp. 947–951, 2001.

[25] E.J. Barth, "A cooperative control structure for UAV's executing a cooperative ground moving target engagement (CGMTE) scenario," in *Proceedings of the American Control Conference*, 2006, pp. 2183–2190.

[26] D. Galzi and Y. Shtessel, "UAV formations control using high order sliding modes," in *Proceedings of the American Control Conference*, 2006, pp. 4249–4254.

[27] H.K. Khalil, *Nonlinear Systems*, Upper Saddle River, NJ: Prentice Hall, 2002.

[28] R. Olfati-Saber and R.M. Murray, "Distributed structural stabilization and tracking for formations of dynamic multi-agents," in *Proceedings of the 41st IEEE Conference on Decision and Control*, 2002, vol. 1, pp. 209–215.

[29] R.W. Brockett, *Asymptotic stability and feedback stabilization*, Ft. Belvoir: Defense Technical Information Center, 1983.

[30] C.C. de Wit and O.J. Sørdalen, "Exponential stabilization of mobile robots with nonholonomic constraints," *IEEE Transactions on Automatic Control*, vol. 37, no. 11, pp. 1791–1797, 1992.

[31] A. Astolfi, "Exponential stabilization of a wheeled mobile robot via discontinuous control," *Journal of Dynamic Systems, Measurement, and Control*, vol. 121, pp. 121–126, 1999.

[32] E. Badreddin and M. Mansour, "Fuzzy-tuned state feedback control of a nonholonomic mobile robot," *IFAC World Congr*, vol. 6, pp. 577–580, 1993.

[33] M. Lal, "Motion planning algorithm for a group of mobile agents," Ph.D. Dissertation, Texas A&M University, College Station, Texas, 2008.

VITA

Sang-Bum Woo was born in Korea. He received his B.S. in Mechanical Engineering from the Yonsei University, Seoul in Feb, 1999 and his M.S. in Mechanical Engineering from the Texas A&M University, College Station in May, 2002. In Sep, 2002 he started his Ph.D. in Mechanical Engineering at the Texas A&M University, and he received his Ph.D. in Dec, 2008. His research interests include multi robot system control and stability analysis in nonlinear system.

Sang-Bum Woo may be reached at Samsung Electronics Co., Ltd., 416, R4 Bldg, Maetan-3Dong, Yeungtong-Gu Suwon city, Gyeonggi-Do, Korea 442-742. His email is woosangbum@gmail.com.

The typist for this dissertation was Sang-Bum Woo.